

**Processing of Alumina Powder into Ceramic Foam Materials by Impregnating  
Polyurethane Sponge with Bonded Ceramic Slurry**

by

Mohd Zikri Bin Ahmad Abustaman  
ID: 8032

Dissertation submitted in partial fulfillment of  
the requirements for the  
Bachelor of Engineering (Hons)  
(Mechanical Engineering)

JULY 2008

Universiti Teknologi Petronas  
Bandar Seri Iskandar  
31750 Tronoh  
Perak Darul Ridzuan

## **CERTIFICATION OF APPROVAL**

### **Processing of Alumina Powder into Ceramic Foam Materials by Impregnating Polyurethane Sponge with Bonded Ceramic Slurry**

by

Mohd Zikri Bin Ahmad Abustaman

A project dissertation submitted to the  
Mechanical Engineering Programme  
Universiti Teknologi PETRONAS  
in partial fulfilment of the requirement for the  
BACHELOR OF ENGINEERING (Hons)  
(MECHANICAL ENGINEERING)

Approved by,

---

(AP. Dr Bambang Ariwahjoedi)

UNIVERSITI TEKNOLOGI PETRONAS

TRONOH, PERAK

July 2008



## **CERTIFICATION OF ORIGINALITY**

This is to certify that I am responsible for the work submitted in this project, that the original work is my own except as specified in the references and acknowledgements, and that the original work contained herein have not been undertaken or done by unspecified sources or persons.

---

MOHD ZIKRI BIN AHMAD ABUSTAMAN

## ABSTRACT

Ceramic foams have an interesting combination of properties, such as low weight, high temperature stability, high permeability, high porosity, low thermal conductivity, and low heat capacity. These properties have lead to a diverse range of applications, such as metal melt filtration, ion-exchange filtration, heat exchangers catalyst support, and refractory linings. Most of the production routes to such materials are via expensive sol-gel or chemical vapor deposition (CVD) technique. For that reason, the objective of this research is to develop a simple and economical method to synthesize and subsequently characterize ceramic foam using Alumina processed via powder routes, by an aid of Polyurethane (PU) sponge as template. The fundamental components for the process are; ceramic (Alumina powder,  $\text{Al}_2\text{O}_3$ ), available foam (Polyurethane, PU-sponge) as a template, Carboxyl Methyl Cellulose (CMC) as an organic binder, Sodium Meta Silicate ( $\text{Na}_2\text{O} \cdot \text{SiO}$ ) as a sintering aid, and distilled water ( $\text{H}_2\text{O}$ ) as a wetting agent. The process starts with selection of the template from four different samples of PU sponge by using various analysis such as TGA and SEM-EDS analysis. Next is the production of ceramic slurry by mixing the optimum compositions of each material in a ball mill. The resulting slurry is then impregnated into cut of the selected PU sponge in which a way that it carry a high loading. Subsequent to that, the impregnated foam will undergo drying process to remove the water before the organic additives were removed by calcination process. The impregnated foam will then subsequently undergo firing and re-firing (sintering process) with slow scheduled to get the foam microstructure and to burn out all the remaining processing additives. The resulting ceramic foam will then be characterized in terms of its porosity, pore structure, pore individual shape, density, linear and volume shrinkages, crystallinity and crushing strength.

*Keywords:* Refractory Ceramic foams, Alumina powder, Polyurethane (PU) foam, Carboxyl Methyl Cellulose (CMC), Sodium Meta Silicate, and water.

## **ACKNOWLEDGEMENTS**

The author wishes to take the opportunity to express his utmost gratitude to the individual that have taken the time and effort to assist the author in doing the project. Without the cooperation of these individuals, no doubt the author would have faced some minor complications through out the end of the first phase of the course.

First and foremost the author's utmost gratitude goes to the author's supervisor, Associate Professor Dr. Bambang Ariwahjoedi. Without his guidance and patience, the author would not be succeeded to work out the project. To his co-supervisor, Associate Professor Dr. Faiz Ahmad for his support. To the Final Year Research Project Coordinator, Professor Vijay, Dr. Sri Putri and Mrs Rosmawati for provide him with all the initial information required to begin the project.

To the technicians in Mechanical Engineering:

1. Mohamed Faisal Bin Ismail
2. Irwan Bin Othman

and the technicians in Chemical Engineering Department, thank you for assisting the author in doing his project.

To all individuals that has helped the author in any way, but whose name is not mentioned here, the author thank you all.

## TABLE OF CONTENTS

<b>CERTIFICATION</b>	.	.	.	.	.	.	.	i
<b>ABSTRACT</b>	.	.	.	.	.	.	.	iii
<b>ACKNOWLEDGEMENT</b>	.	.	.	.	.	.	.	iv
<b>LIST OF FIGURES</b>	.	.	.	.	.	.	.	vii
<b>LIST OF TABLES</b>	.	.	.	.	.	.	.	viii
<b>LIST OF APPENDICES</b>	.	.	.	.	.	.	.	ix
<b>LIST OF ABBREVIATIONS</b>	.	.	.	.	.	.	.	x
<b>CHAPTER 1:</b>	<b>INTRODUCTION</b>	.	.	.	.	.	.	1
1.1	Project Background	.	.	.	.	.	.	1
1.2	Problem Statement	.	.	.	.	.	.	2
	1.2.1 Problem Identification	.	.	.	.	.	.	2
	1.2.2 Significance of Project	.	.	.	.	.	.	2
1.3	Objectives and Scope of Study	.	.	.	.	.	.	2
	1.3.1 Relevancy of Project	.	.	.	.	.	.	3
1.4	Feasibility of Project	.	.	.	.	.	.	3
<b>CHAPTER 2:</b>	<b>LITERATURE REVIEW/THEORY</b>	.	.	.	.	.	.	4
2.1	Literature Review	.	.	.	.	.	.	4
	2.1.1 Ceramic Foam	.	.	.	.	.	.	4
	2.1.1.1 Ceramic Foam Applications	.	.	.	.	.	.	5
	2.1.1.2 Ceramic Foam Manufacturing.	.	.	.	.	.	.	5
2.2	Ceramic Foam Properties	.	.	.	.	.	.	7
	2.2.1 Mechanical and Thermal Properties	.	.	.	.	.	.	8
	2.2.2 Creep Rate and Time to Failure.	.	.	.	.	.	.	9
	2.2.3 Pressure Drop	.	.	.	.	.	.	10
	2.2.4 Crushing strength	.	.	.	.	.	.	11
<b>CHAPTER 3:</b>	<b>METHODOLOGY/PROJECT WORK</b>	.	.	.	.	.	.	13
3.1	Methodology	.	.	.	.	.	.	13
3.2	Materials	.	.	.	.	.	.	14
	3.2.1 Ceramic	.	.	.	.	.	.	15
	3.2.2 Foam	.	.	.	.	.	.	15
	3.2.3 Processing Additives	.	.	.	.	.	.	15
	3.2.3.1 Liquid/Solvent	.	.	.	.	.	.	16
	3.2.3.2 Binders	.	.	.	.	.	.	16
	3.2.3.3 Sintering Aid	.	.	.	.	.	.	17
3.3	Tools and Equipment	.	.	.	.	.	.	17
	3.3.1 Thermo gravimetric Analysis (TGA)	.	.	.	.	.	.	17

	3.3.2 Scanning Electron Microscope-Energy Dispersive Spectrometer (SEM-EDS)	18
3.4	Synthesis Process	18
	3.4.1 Ceramic Slurry Preparation	18
	3.4.1.1 Composition Calculation	19
	3.4.2 Impregnation Process	19
	3.4.3 Drying and Calcination Process.	20
	3.4.4 Sintering/Firing Process.	20
	3.4.5 Characterization Process	21
	3.4.5.1 Density	21
	3.4.5.1.1 Bulk density, $\rho_1$	21
	3.4.5.1.2 Apparent density, $\rho_2$	22
	3.4.5.1.3 True density, $\rho_3$	22
<b>CHAPTER 4:</b>	<b>RESULT AND DISCUSSION</b>	24
4.0	Result	24
4.1	Template selection	24
	4.1.1 TGA analysis	24
	4.1.2 SEM-EDS analysis	25
4.2	Optimum Composition	27
4.3	Firing Schedule	28
4.4	Sintering	30
4.5	Characteristic	31
	4.5.1 Microscopic analysis	31
	4.5.2 Pore linear density	33
	4.5.3 Density	33
	4.5.3.1 Bulk density, $\rho_1$	33
	4.5.3.2 Apparent density, $\rho_2$	34
	4.5.3.3 True density, $\rho_3$	34
	4.5.4 Product shrinkage	34
	4.5.4.1 Linear shrinkage	34
	4.5.4.2 Bulk volume shrinkage	35
	4.5.5 Crystalline analysis	35
	4.5.6 Crushing strength	36
4.6	Discussion	37
<b>CHAPTER 5:</b>	<b>CONCLUSION AND RECOMMENDATION</b>	41
5.0	Summary/Conclusion	41
5.1	Recommendation	42
<b>REFERENCES</b>		43
<b>APPENDICES</b>		46

## LIST OF FIGURES

Figure 1	TiO <sub>2</sub> ceramic foam . . . . .	7
Figure 2	Pressure drop of a sphere packed bed. . . . .	11
Figure 3	Typical stress-strain plot for pore ceramic . . . . .	12
Figure 4	Summary of process flow for sponge replication technique. . . . .	13
Figure 5	Sample dimension . . . . .	22
Figure 6	Apparent density method . . . . .	22
Figure 7	Pycnometer . . . . .	23
Figure 8	TGA result: All Samples . . . . .	25
Figure 9	SEM image of sample 2 . . . . .	26
Figure 10	Weight versus solid contents of ceramic foam . . . . .	27
Figure 11	TGA curve for the complete mixture . . . . .	28
Figure 12	Dwell range estimation of the highest sintering temperature. . . . .	29
Figure 13	Overall firing schedule . . . . .	30
Figure 14 a	Sample before sintering . . . . .	30
Figure 14 b	Sample after sintering. . . . .	30
Figure 15	SEM image of ceramic foam . . . . .	31
Figure 16	Schematic of pore mechanism of ceramic foam . . . . .	32
Figure 17	EDS test of the final product . . . . .	33
Figure 18	Crystallinity analysis using XRD . . . . .	36
Figure 19	Stress vs strain graph for the final product . . . . .	37
Figure A1	Project Gantt chart. . . . .	47
Figure A2	Process flow for Foaming technique . . . . .	48
Figure A3	Mechanism of vacuum impregnation technique . . . . .	49
Figure A6a	TGA result: Sample 1 . . . . .	53
Figure A6b	TGA result: Sample 2 . . . . .	53
Figure A6c	TGA result: Sample 3 . . . . .	54
Figure A6d	TGA result: Sample 4 . . . . .	54
Figure A7a	SEM image of sample 2 . . . . .	55
Figure A7b	SEM image of sample 3 . . . . .	55
Figure A7c	SEM image of sample 4 . . . . .	56
Figure A8	Practiced firing schedule for solid Alumina ceramic . . . . .	57

## LIST OF TABLES

Table 1	Constants of the Tetrakaidecahedron unit cell.	.	.	8
Table 2	Mechanical and thermal properties of low density open cell foam			9
Table 3	Equipments and tools required in the experiment	.	.	17
Table 4	TGA analysis result	.	.	25
Table 5	Composition of each sample using EDS	.	.	26
Table 6	Optimum composition of 66% solid contain	.	.	28
Table 7	Chemical composition of the final product	.	.	33

## LIST OF APPENDICES

Appendix 1	Project Gantt chart . . . . .	47
Appendix 2	Process flow for foaming technique . . . . .	48
Appendix 3	Vacuum impregnation technique for impregnation process	49
Appendix 4	Manual compression technique for impregnation process	50
Appendix 5	Four different types of available PU sponge . . . . .	52
Appendix 6	TGA result for each sample of PU sponges . . . . .	53
Appendix 7	SEM images of PU-sponge sample . . . . .	55
Appendix 8	Firing schedule for Alumina . . . . .	57



## **LIST OF ABBREVIATIONS**

PU	Polyurethane
CMC	Carboxyl Methyl Cellulose
SMS	Sodium Meta Silicate
TGA	Thermo gravimetric Analysis
FT-IR	Fourier Transformed-Infrared Spectroscopy
PPI	Pore per inch
SEM	Scanning Electron Microscopy
CVD	Chemical Vapor Deposition
XRD	X-Ray Diffraction

# **CHAPTER 1**

## **INTRODUCTION**

### **1.0 INTRODUCTION**

The designation of this final year project is processing of Alumina powder into ceramic foam materials by impregnating Polyurethane sponge with bonded ceramic slurry. This chapter will describe the background of study, problem statement, objective and the scope of work.

### **1.1 Project Background**

Ceramic foam and cellular materials are being used in a wide variety of industries and are finding ever growing number of applications. The ceramic foam can be used not only for thermal insulation, but for a variety of other applications such as acoustic insulation and adsorption of environmental pollutants. Over the past decade, advances in manufacturing of cellular materials have resulted in ceramics with highly uniform interconnected porosities ranging in size from a few  $\mu\text{m}$  to several mm. These relatively new ceramic foam materials have a unique set of thermo-mechanical properties, such as excellent thermal shock resistance and high surface to volume ratios. Based on new advances in processing ceramic foams, this project suggests the development of ceramic foams or cellular ceramics for producing ceramic foam materials by using ceramics processing via sponge replication technique. The possible outcomes from this project will be a simple and economical way in producing ceramic foam materials that can be implicated for an industrial usage.

## **1.2 Problem Statement**

Most of the production routes of ceramic foams are using expensive sol-gel, chemical vapor deposition (CVD) or foaming techniques as the processing involve complex procedures since the materials used need careful handlings which certainly need multifarious equipments. A simple and cheap way to synthesize ceramic materials with such a microstructure is always deficiently needed and is the aims of this project.

### **1.2.1 Problem Identification**

Identification and developing of a correct method and experimental procedures on processing powder routes of ceramic into ceramic foam materials is crucial in this project. Therefore, thorough research and trial-and-error methods must be done to ensure the project will be a success. Apart from that, selection of processing additives also vital in this project as the availability and cost of each additive must be considered.

### **1.2.2 Significance of Project**

The significance of this project is that in the future, this project could be a benchmark of one of the simple and efficient method to produce ceramic foam materials for an industrial usage. The research could also be expanded on the other methodology and materials in producing the ceramic foam materials.

## **1.3 Objectives and Scope of Study**

The main objective of this project is to synthesize and subsequently characterize Alumina ( $\text{Al}_2\text{O}_3$ ) ceramic foam processed via powder routes, by an aid of Polyurethane sponge as template. The synthesis will be done by an aid of several processing additives such as Carboxyl Methyl Cellulose (CMC) as binding additives, Sodium Meta Silicate ( $\text{Na}_2\text{O} \cdot \text{SiO}$ ) as a sintering aid and distilled water ( $\text{H}_2\text{O}$ ) as a liquid additive.

### **1.3.1 Relevancy of Project**

This project is an approach to materials science and ceramics engineering, providing an understanding of the scientific principles and technology of ceramics processing as it applies to the development and production of new advanced ceramics technology.

### **1.4 Feasibility of Project**

The scope of the project is divided into two phases that is executed in an overall duration of 11 months. The first phase is the synthesis process while the second phase is the characterization process. For the first phase of this project, the focus is on the synthesis part to produce the ceramics foam materials. This synthesis part includes the foam selection, ceramic slurry preparation, determination of an optimum composition, impregnation process, and sintering process in sequence. For the second phase, the focus is on characterization aspects. This characterization process includes measurement of the final product's density, porosity, pore structure, pore individual shape, density, linear and volume shrinkages, crystallinity and crushing strength. The overall project Gantt chart is shown in figure A1 of appendix 1.

## **CHAPTER 2**

### **LITERATURE REVIEW/THEORY**

#### **2.0 LITERATURE REVIEW/THEORY**

##### **2.1 Literature Review**

This chapter will describe the literature review and theory on the subjects of the study which are taken from 6 main books, 27 articles and 2 from internet sources. This chapter will include; discussion on ceramic foam, the applications of ceramic foam, how is the ceramic foam being manufactured, and what are the properties of the ceramic foam.

##### **2.1.1 Ceramic Foam**

Ceramic foams have a remarkable combination of properties, such as low weight, high temperature stability, high permeability, high porosity, low thermal conductivity, and low heat capacity which have led to a diverse range of applications, such as metal melt filtration, ion-exchange filtration, heat exchangers, catalyst support, refractory linings, thermal protection systems, diesel soot traps, flame rectifiers, and solar radiation collectors (Nangrejo et al, 2001, Fend et al, 2004). Recently, the biotechnology and biomedical industries are employing ceramic foams made of hydroxyapatite, which can simulate bone and bio implants (Hutmacher, 2000, Sepulveda & Binner, 1999). Most of the new applications have been made possible because of advances in manufacturing ceramic foams with highly tailored pore morphologies.

### **2.1.1.1 Ceramic Foam Applications**

Engineered foams have cellular structures which are categorized as either open cell or closed cell foams. Foam consists of an assembly of irregularly shaped prismatic or polyhedral cells connected to each other with solid edges (open cell) or faces (closed cell). Engineered foams have been manufactured from polymers, metals, glasses, and ceramics. Ceramic foams are porous brittle materials with closed, fully open, or partially interconnected porosity. First, some of ceramic foam applications are highlighted followed by a discussion of various manufacturing processes. Ceramic foams offer a unique combination of properties, such as low density, high surface area to volume ratio, high stiffness to weight ratio, low thermal and electrical conductivity, and highly localized strain and fracture characteristics (Nangrejo et al, 2001, Fend et al, 2004). Ceramic foams have a very high thermal shock resistance and thus open cell foam is used to spread flames, fuels, or coolants uniformly (Muir et al, 1993, Fend et al, 2004). Closed cell ceramic foams are mostly used for fire protection and thermal insulation materials. Open cell ceramic foams are used for a very wide range of applications. The excellent thermal shock resistance facilitates their use for metal melt filtration (Montanaro, 1998) and Diesel engine exhaust filters (Montanaro, 1999, Inui & Ottawa, 1986). Ceramic foam filters improve molten metal casting quality by removing non metallic inclusions. These filters must withstand thermal shock and be stable against chemically reactive metals at elevated temperatures. Combustion in porous media is an intense area of research because of flame stabilization, improved burning velocity, and reduction in NO<sub>x</sub> emission (Russo et al, 2003, Lammers & De Goey, 2003). Ceramic foams are employed in catalytic combustion devices and in a variety of catalysis reactors (Richardson et al, 2000). Ceramic foams are also being developed and employed for solar based processes, either direct CO<sub>2</sub>-CH<sub>4</sub> reforming (Muir, 1993) or volumetric receivers for concentrated solar radiation (Fend et al, 2004). More recently porous ceramic materials are finding applications as bio-resorbable macroporous scaffolds for bone tissue engineering. The high interconnectivity of porous ceramics ensures the transport of nutrients and metabolic waste, as well as large surface areas for tissue attachment and growth (Hutmacher, 2000, Montanaro, 1998, Almiralla et al, 2004).

### **2.1.1.2 Ceramic Foam Manufacturing**

Ceramic foam manufacturing techniques can be classified into three general categories: chemical vapour deposition (CVD), foaming agents, or space holder method.

The CVD was first developed in the early 1960s (Schwartzwalder & Soners, 1963). CVD technique is using a complex chemical reaction in developing the high density struts as well as developing a well distributed pore to the ceramic (Gibson & Ashby, 1999, Montanaro, 1998, Saggio-Woyansky, 1992, Sherman et al, 1991). Figure 1 shows an example of a  $\text{TiO}_2$  foam made by CVD technique (Haugen et al, 2004).

The second technique is based on gas bubbles in preceramic melts (Gibson & Ashby, 1999, Sepulveda & Binner, 1999, Montanaro, 1998, Zeschky et al, 2003). Gas evolving constituents are added to the melt. During the treatment bubbles are generated, causing the material to foam. This process was introduced in 1973 by Sunderman and Viedt. Foaming uniformity and cell geometry can be adjusted by careful selection of surfactants and foaming agents (Colombo & Modesti, 1999, Nangrejo & Edirisinghe, 2002). The process flow of this technique can be seen in figure A2 in appendix 2.

The third technique is based on a space holder concept. For example, sodium chloride is sintered and compacted to form a porous space holder, which is infiltrated with polycarbosilane. The salt is then dissolved and a polymer foam remains, which is then pyrolyzed to form the SiC foam (Fitzgerald & Mortensen, 1995). Qian (2004) made highly porous SiC ceramic with wood-like microstructure and porosity by infiltrating wood with silica sol-gel. The resulting porous SiC morphology resembles a wood microstructure.

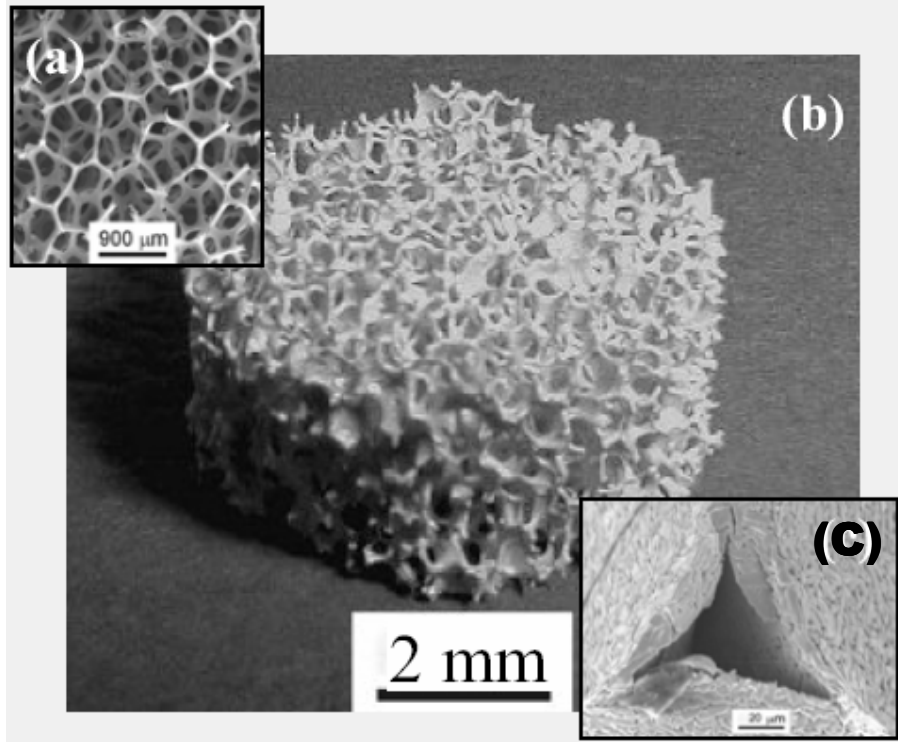


Figure 1:  $\text{TiO}_2$  ceramic foam: (a) fully reticulated polyester polyurethane foam with 45 ppi; (b)  $\text{TiO}_2$  foam, (c) hollow  $\text{TiO}_2$  foam ligament. (Haugen, 2004)

## 2.2 Ceramic Foam Properties

Typically, open cell ceramic foams exhibit high porosities (70–90%) with non uniform spherical-like cells connected to each other by ligaments. The tortuosity of the foam is characterized in terms of the pore diameter,  $d_p$ , or pore per inch (PPI) density. Typical pore diameters range between 0.01 to 2 mm, although recently open cell microcellular SiOC foams with cell sizes ranging from about 1 to 100 microns have been manufactured (Colombo & Modesti, 1994). In isotropic foams, typical pore densities range between 10 to 100 ppi. Figure 1 shows an example of a sponge replicated 40-PPI  $\text{TiO}_2$  foam. The tetracadehedron is the most common unit cell structure of open-cell foams, consisting of 14 faces, 36 edges and 24 vertices. Table I lists the geometric constants of a tetrakaidehedron unit cell. The interconnecting



struts provide an enormous surface area per unit volume,  $S_v$ . In 10 to 65 PPI poredensities,  $S_v$  varies from  $1.71 \times 10^4$  to  $6.84 \times 10^4$  m<sup>2</sup>/m (solid) (Montanaro, 1999), which is equivalent to that of spherical packed beds with diameters ranging 0.05 to 0.34 mm. (Richardson et al, 2000). An important property of any cellular solid is its relative density,  $\rho^*/\rho_s$ ; where  $\rho^*$  is the density of the cellular solid and  $\rho_s$  is the density of the solid from which the foam is made. In general, a relative density of 0.3 is the cut-off value between cellular solids (foams) and porous materials. For low density foams the relative density can be expressed in terms of unit cell geometric constants given in Table I.

Table 1: Constants of the tetrakaidecahedron unit cell. (Gibson & Ashby, 1999, Richardson et al, 2000)

Property	Symbol	Formula
Pore diameter	$d_p$	Measured
Solid porosity	$p$	Measured
Hexagonal side	$l$	$0.5498d_p/[1-0.97(1-p)^{0.5}]$
Strut thickness	$t_s$	$0.971(1-p)^{0.5}l$
Cell volume	$V_c$	$11.31x l^3$
Strut surface area	$S_s$	$36t_sx l$
Surface area/vol.	$S_v$	$S_s/[V_c(1-p)]$

### 2.2.1 Mechanical and Thermal Properties

The mechanical properties of open cell foams, e.g., stiffness ( $E^*$ ), the elastic collapse stress ( $\sigma_{el}^*$ ), the plastic collapse stress ( $\sigma_{pl}^*$ ), the crush strength ( $\sigma_f^*$ ), and the fracture toughness ( $KIC^*$ ) are summarized in Table 2. Foams made of engineering ceramics such as alumina offer comparatively high strengths approximately up to 80 MPa crush strength and 25 MPa modulus of rupture (Gibson & Ashby, 1999, Sherman et al, 1991).

Table 2: Mechanical and thermal properties of low density open cell foam (Gibson & Ashby, 1999, Maiti et al, 1984).

Property	Formula
Density	$\rho^* / \rho_s = C_1 (t/l)^2$
Stiffness	$E^*/E_s \approx 1.0 (\rho^* / \rho_s)^2$
Elastic Collapse Stress	$\sigma_{el}^*/E_s \approx 0.05 (\rho^* / \rho_s)^2$
Plastic Collapse Stress	$\sigma_{pl}^* / \sigma_y \approx 0.3 (\rho^* / \rho_s)^{3/2}$
Crushing Strength	$\sigma_f^* / \sigma_{fs} \approx 0.2 (\rho^* / \rho_s)^{3/2}$
Fracture Toughness	$K_{IC}^* / \sigma_{fs} \approx 0.65 \sqrt{\pi l} (\rho^* / \rho_s)^{3/2}$
Creep	$\epsilon_f'^* / \epsilon_0' \approx (0.6/(n+2)) (1.7(2n+1) \sigma^* / n \sigma_0) (\rho_s / \rho^*)^{(3n+1)/2}$
Thermal Conductivity	$K^*/K_s \approx 0.35 (\rho^* / \rho_s)$

### 2.2.2 Creep Rate and Time to Failure

Compressive creep of open-cell Al<sub>2</sub>O<sub>3</sub> foam was measured for temperatures between 1200°C and 1500°C (Andrews et al, 1999). The creep behavior of the ceramic foam was very similar to that of dense alumina except at much lower stresses. For strain rates between 10<sup>-8</sup> and 10<sup>-6</sup> s<sup>-1</sup> creep occurred by diffusional flow for stresses in the range 20-100 kPa. The activation energy for steady state creep was 504 kJ/mol, which is typical for creep of dense alumina. The onset of tertiary creep was associated with the formation of creep cracks in the struts subjected to bending. For diffusional flow the parameter, n, of the creep equation (Table 2) is unity and the steady state creep then becomes (Goretta et al, 1990) as the equation 1 below:

$$\epsilon_f'^* \approx A \sigma^* / \sigma_s (\rho^* / \rho_s)^2 \exp (-Q/RT) \quad (1)$$

Where  $\epsilon_f'^*$  is the foam steady state creep rate,  $\sigma^*$  is the foam crushing strength,  $\rho^*$  is foam density, and Q is the foam activation energy; and  $\sigma_s$ ,  $\rho_s$  are solid material values. Open cell foam is thus expected to have the same stress dependence and activation energy as the dense material, with the difference of a -2 power of the relative density  $(\rho^* / \rho_s)^{-2}$ . For alumina foam with densities less than 30% the steady

state creep rate at strain rates between  $10^{-8}$  and  $10^{-6}$  s $^{-1}$  in a temperature range of 1200- 1500°C was found to be as the equation 2 below:

$$\dot{\epsilon}_f^* \approx A \sigma^{1+0.1} \exp (-504+20\text{kJmol}^{-1}/RT) (\rho_s / \rho^*)^{1.8} \quad (2)$$

Creep rates larger than 6% to 9% resulted in accelerated creep that caused creep cracks in individual ligaments. The analysis showed that the primary deformation mode in these ceramic foams was consistent with strut bending. In a review of creep in cellular solids, Andrews et al. (1999) examined the behavior of metallic aluminum foams. The failure times of ceramic foams is well described in the equation 3 below with the Monkman-Grant relationship (Goretta et al, 1990):

$$\text{Log } t_r + m \log \dot{\epsilon} = B \quad (3)$$

Where B and m are density dependent constants. Thus lifetime predictions become possible for known creep rates.

### 2.2.3 Pressure Drop

Richardson et al. (2000) compared the pressure drop of a bed of glass spheres to that of alumina foam for catalytic reactor applications. Both had similar geometric surface areas. The glass spheres had a diameter of 0.5 mm, a porosity of 0.416, and a surface area of  $0.582 \times 10^4$  m $^2$ /m $^3$ . Equivalent alumina foam was chosen with a pore density of 30 PPI, which translates into a porosity of about 0.874 with a bed equivalent geometric surface area of  $0.423 \times 10^4$  m $^2$ /m $^3$ . Although surface areas are similar between the sphere packed bed and the foam, the larger porosity of the foam results in a reduction in pressure drop of about a factor of 16 at high velocities. Figure 2 demonstrates the reduced pressure drop of ceramic foam catalyst structures compared with sphere packed beds.

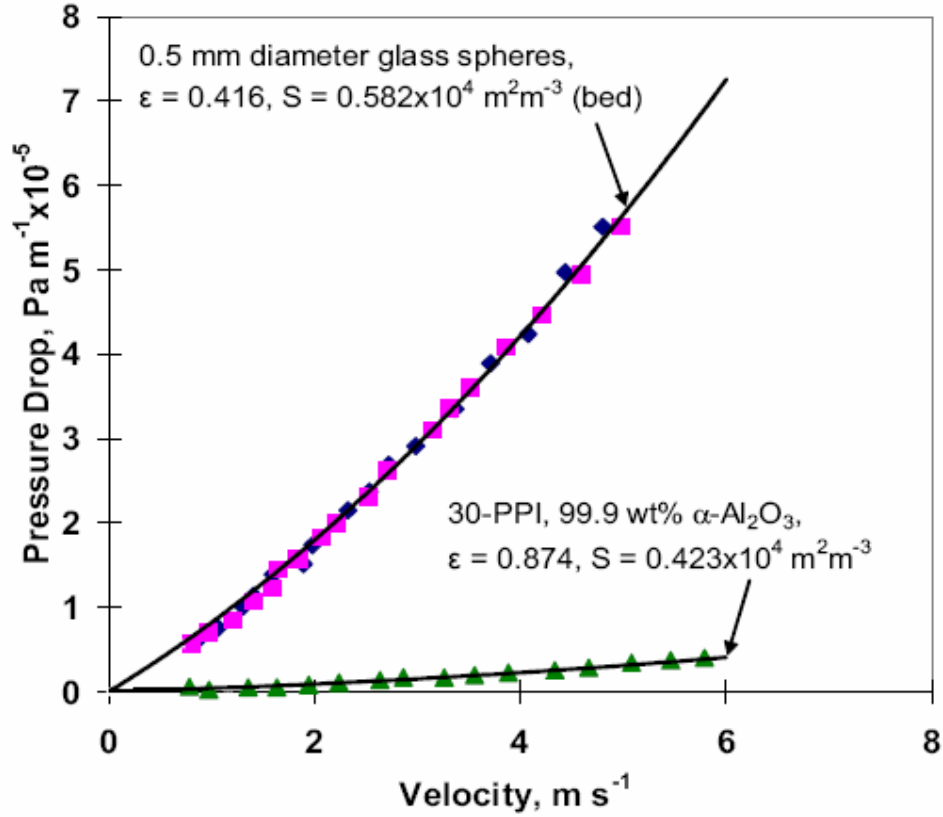


Figure 2: Pressure drop of a sphere packed bed (glass beads ~0.5 mm diameter) and a 30-PPI, 99.5 wt%  $\alpha\text{-Al}_2\text{O}_3$  foam with comparable geometric surface areas.

(Richardson, 2000)

#### 2.2.4 Crushing strength

As depicted in the typical stress-strain plot in figure 3, when a load is applied to a foam structure, the foam will initially yield elastically. The slope of this initial stress / strain curve is the defined by the stiffness of the foam. The stiffness or Young's Modulus of a foam structure is a function of the solid material modulus and the square of the foam structure relative density in the rather simple and elegant equation:

$$\text{Modulus}_{\text{foam}} = \text{Modulus}_{\text{solid}} \times \text{relative density}^2 \quad (4)$$

Where;

$\text{Modulus}_{\text{foam}}$  = Young's Modulus of the isotropic foam structure

$\text{Modulus}_{\text{solid}} = \text{standard Young's Modulus of the solid strut material}$

Relative density = % foam relative density in decimal form, i.e. 1% = .1

When a load is applied to a foam structure, it will initially yield elastically in accord with the Young's modulus equation (equation 4). However, at approximately 4-6% of strain, depending on the sample size, the foam structure will begin to buckle and collapse continuously at a relatively constant stress. Depending upon the initial relative density of the foam, this constant collapse will proceed to approximately 50-70% of strain. At that point, the stress / strain curve will begin to rise as the compressed foam enters the “densification” phase. The point in the stress / strain curve where it transitions from the elastic to plastic deformation phase defines the “crush strength” of the foam. This is an important mechanical parameter as it is obviously essential to remain below that level for any structure that is being designed to maintain its shape under design load.

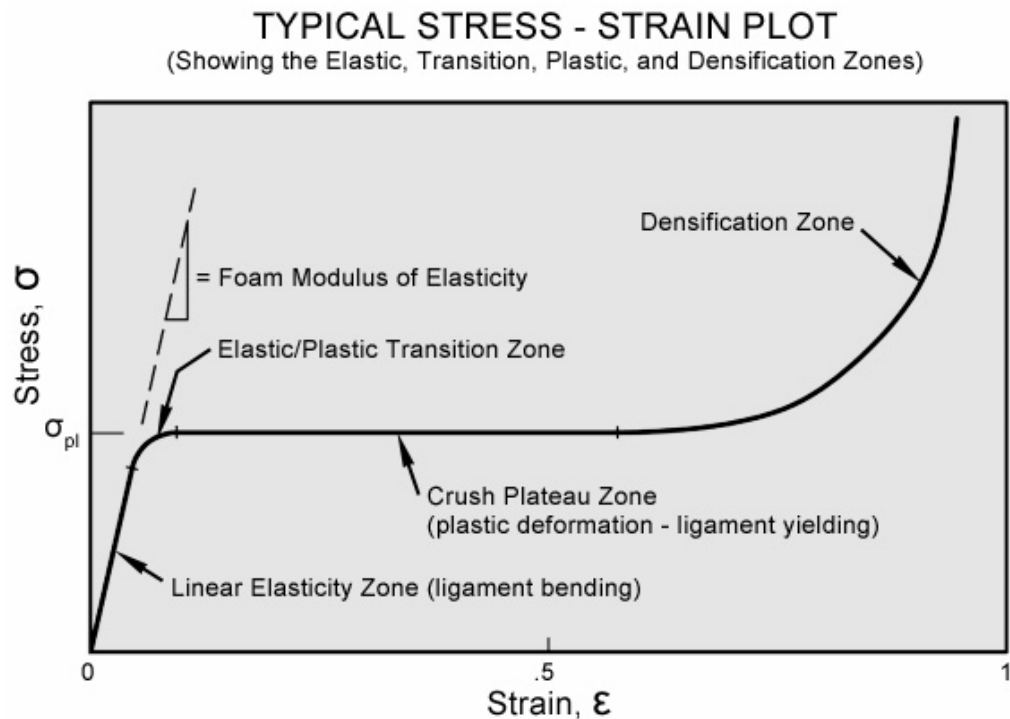


Figure 3: Typical stress-strain plot for pore ceramic. (Richardson, 2000)

## CHAPTER 3

### METHODOLOGY/PROJECT WORK

#### 3.0 METHODOLOGY/ PROJECT WORK

##### 3.1 Methodology

In this project, the processing of the Alumina ceramic foam materials is using sponge replication technique whereby the available Polyurethane sponge is used directly as a template for the ceramic to become ceramic foam. The summary of the process flow is visualized in figure 4 below:

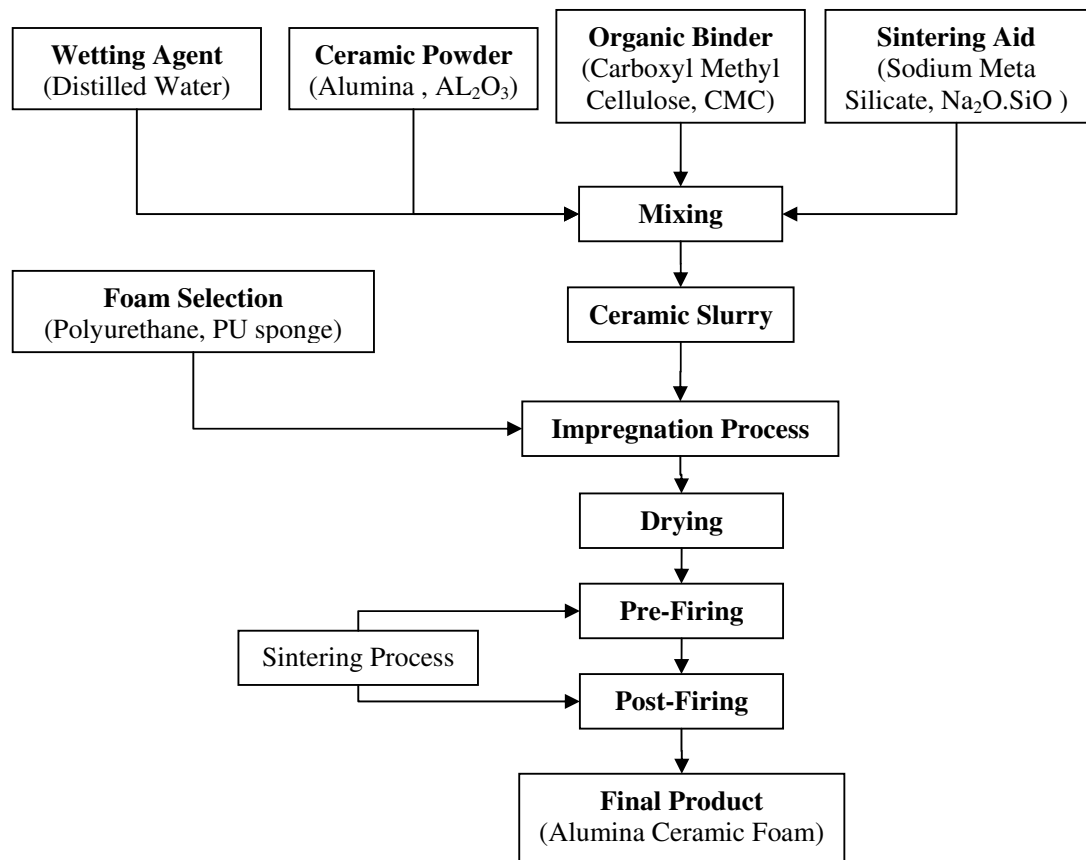


Figure 4: Summary of process flow for sponge replication technique.

The detailed explanation of the procedures in this technique is as follow:

1. Polyurethane sponges are tested using TGA tool in order to select the best foam to be used as the template of the ceramic foam.
2. The selected PU sponge will then be examined using SEM-EDS tools to identify the pore structure and its compositions.
3. Ceramic slip is produced by ball milling Alumina powder with Carboxyl Methyl Cellulose (CMC) binder and the other processing additives such as distilled water as a liquid to wet the medium, and Sodium Meta Silicate (SMS) as a sintering aid.
4. The resulting slurry is then impregnated into cut of the selected Polyurethane foam in such a way that it carries a high loading. The impregnation method that is used is a manual compression method.
5. The impregnated foam will then undergo a drying process to eliminate the water inside the mixture.
6. The dried foam will then subsequently fire with slow scheduled to get the foam microstructure.
7. The fired ceramic foam will be re-fired to ensure that all foam is eliminated as well as to remove most of the processing additives.
8. The resulting foam will then be characterized in terms of its density, pore structure, PPI, product shrinkage, crystallinity and crushing strength.

The project activities are divided into two phases that is executed in an overall duration of 11 months. The first phase is the synthesis process while the second phase is the characterization process. For the first phase of this project, the focus is on the synthesis part to produce the ceramics foam materials. This synthesis part includes the foam selection, ceramic slurry preparation, determination of an optimum composition, impregnation process, and sintering process in sequence. For the second phase, the focus is on characterization aspects. This characterization process includes measurement of the final product's density, porosity, pore structure, pore individual shape, density, linear and volume shrinkages, crystallinity and crushing strength. The overall project Gantt chart is shown in figure A1 of appendix 1.

### 3.2 Materials

The essential materials for the process using this sponge replication technique can be divided into three main groups;

1. Ceramic
2. Foam
3. Processing additives; this consists of the following;
  - i. Organic binder
  - ii. Sintering aid
  - iii. Wetting agent.

#### 3.2.1 Ceramic

In this project the ceramic that is used is Aluminium Oxide in form of powder. It is an amphoteric oxide of aluminium with the chemical formula  $\text{Al}_2\text{O}_3$ . It is also commonly referred to as alumina or aloxite (Ceramic Materials, 2008). Alumina is mainly useful because of the size, distribution, and homogeneity of the porosity that can be formed and the easiness of processing (Bagwell & Messing, 1996). It is used as an abrasive due to its hardness and as a refractory material due to its high melting point (Barsoum, 2003). Some of the physical and chemical properties of Alumina are as follows:

- Appearance: Solid, white powder.
- Odor: Odorless.
- Solubility: Insoluble in water.
- % Volatiles by volume @ 21°C (70°F): 0
- Boiling Point: 2977 °C (5391 °F)
- Melting Point: 2050 °C (3722 °F)

#### 3.2.2 Foam

In this project, the method of producing the refractory ceramic foam is via sponge replication technique. Within this technique, available Polyurethane sponge is used as a template to set the shape of the final product directly. Polyurethane, commonly abbreviated PU, is a polymer consists of a chain of organic units joined by urethane links. Polyurethane polymers are formed by re-acting a monomer containing at least



two isocyanate functional groups with another monomer containing at least two alcohol groups in the presence of a catalyst. Polyurethanes are in the class of compounds called reaction polymers, which include epoxies, unsaturated polyesters, and phenolics (Gum, 1992, Barsoum, 2003).

### **3.2.3 Processing Additives**

Processing additives are necessary in processing ceramics as they produce the particle dispersion and flow behaviour requisite for forming. Processing additives are added in a small quantity and most are eliminated in a later stage (commonly by pyrolysis) prior to sintering so that they are completely removed and do not appear in the final product (Reed, 1995, Rahaman, 2003). The processing additives can be classified as follows:

1. Liquid/Solvent
2. Binder
3. Sintering Aid

The key to successful in ceramics processing is highly depends on the cautious selection and control of these additives.

#### **3.2.3.1 Liquid/Solvent**

Generally, liquid is an additive used in ceramic processing to wet the ceramic particles. Liquids serve two major functions:

1. Provide fluidity for the powder during forming. (Rahaman, 2003)
2. Serve as solvent for dissolving the additives to be incorporated into the powder, thereby providing a means for uniformly dispersing the additives throughout the powder. (Rahaman, 2003)

In this project, distilled water ( $H_2O$ ) will be used as the liquid additive. The distilled water will be mixed together with the other processing additives during the ceramic slurry preparation and it will be removed during drying process.

### 3.2.3.2 Binders

Binders are typically long chain polymers that serve the primary function of providing strength to the green body by forming bridges between the particles. The strength produced by the binder is important to the formed product for handling works before the product is densified by firing (Reed, 1995). In the slurry preparation process for this project, the binder that will be used is Carboxyl Methyl Cellulose (CMC). CMC is a cellulose type of binder (Reed, 1995) and it is an acid ether derivative of sodium salt cellulose and is utilized as a thickening, emulsifying, and suspending agent (Carboxymethyl Cellulose, 2008).

### 3.2.3.3 Sintering Aid

For the sintering aid, Sodium Meta Silicate 5-Hydrate ( $\text{Na}_2\text{O} \cdot \text{SiO}_2$ ) will be used. This additive is meant to decrease the sintering temperature of the ceramic foam as the melting point of ceramic is very high. Hence, it will make the sintering process become faster and more effective. Sodium silicate is the generic name for a series of compounds derived from soluble sodium silicate glasses. They are water solutions of sodium oxide ( $\text{Na}_2\text{O}$ ) and silicon dioxide ( $\text{SiO}_2$ ) combined in various ratios. Varying the proportions of  $\text{SiO}_2$  to  $\text{Na}_2\text{O}$  and the solids content results in solutions with differing properties that have many diversified industrial applications (Gum, 1992).

## 3.3 Tools and Equipment

The main tools and equipments which are required throughout this project are list down in table 3 according to the specific proposes:

Table 3: Equipments and tools required in the experiment

Propose	Tools and Equipment
PU sponge selection	TGA, SEM-EDS and FT-IR.
Ceramic slurry preparation	Ball mills.
Impregnation process	Vacuum dessicator for vacuum method

	and beaker and pusher for a compression method.
Drying and Firing/Sintering	Electrical oven and electric furnace.
Characterization process	SEM-EDS, optical microscope, Universal Testing Machine, XRD, and Pycnometer.

### **3.3.1 Thermo gravimetric Analysis (TGA)**

Thermo gravimetric analysis (TGA) is an analytical technique used to determine a material's thermal stability and its fraction of volatile components by monitoring the weight change that occurs as a specimen is heated. This tool provides two important numerical pieces of information: ash content (residual mass,  $M_{res}$ ) and oxidation temperature (Rahaman, 2003). TGA tool will be used to analyse the available Polyurethane sponge in order to select the best foam based on the results obtained from this tool.

### **3.3.2 Scanning Electron Microscope-Energy Dispersive Spectrometer (SEM-EDS)**

The scanning electron microscope (SEM) is a type of electron microscope that creates various images by focusing a high energy beam of electrons onto the surface of a sample and detecting signals from the interaction of the incident electrons with the sample's surface. In this project, SEM is used to examine the average pore size of each sponges sample to determine which sample has a suitable pore size so that it can absorb more mixture of the ceramic in the impregnation process later on. Energy Dispersive Spectrometer (EDS) is a chemical analysis of microscopic particles or regions within a sample analyzed in the SEM. EDS micro-analysis is performed by measuring the energy and intensity distribution of X-ray signals generated by a focused electron beam on the specimen. This project used EDS to identify the components of the selected sponge to avoid any redundant reaction occur in the later on process especially in the sintering process. Another tool that will be considered in

determining the components of the sponge is Fourier Transform-Infrared Spectroscopy (FT-IR) machine.

### 3.4 Synthesis Process

#### 3.4.1 Ceramic Slurry Preparation

A ceramic slip is produced by ball milling Alumina powder with CMC, Sodium Meta Silicate and distilled water at a specific composition. The specific composition is referred to an optimum composition. It is obtained by finding the highest weight (gram) with respect to the solid contains. The weight is calculated by finding the different in weight between the burnt samples with unburned samples.

##### 3.4.1.1 Composition Calculation

Formula weight (FW) of solid mixture:

$$FW = \sum (\text{number of atom} \times \text{atomic weight}) \quad (5)$$

1) Sodium Meta Silicate,  $\text{Na}_2\text{O} \cdot \text{SiO}_2$

$$\begin{aligned} FW_{\text{SMS}} &= (2 \times 22.989768) + (3 \times 15.9994) + (1 \times 28.0855) \\ &= 122.063236 \text{ gram/mole} \end{aligned}$$

2) Alumina,  $\text{Al}_2\text{O}_3$

$$FW_{\text{A}} = (2 \times 26.981539) + (3 \times 15.9994) = 101.961278 \text{ gram/mole}$$

Total mole required (y mole) is calculated by setting the desired ratio of the alumina to silica to be 3:2 (60% Alumina and 40% Silica). An example of 10 gram of Alumina and 10 gram of SMS;

$$1) \text{ y mole of 10g Alumina} = (10\text{g}/101.961278\text{g/mole}) = 0.0981 \text{ mole}$$

$$2) \text{ y mole of 10g SMS} = (10\text{g}/122.063236\text{g/mole}) = 0.0819 \text{ mole}$$

Hence mole of Alumina and SMS that are required for the 3:2 ratios is:

$$\Sigma_{\text{mole}} \text{Alumina} = (0.6 \times 0.0981) = 0.05886 \text{ moles} \approx (0.05886 \times 101.961278) \approx 6 \text{ grams}$$

$$\Sigma_{\text{mole}} \text{SMS} = (0.4 \times 0.0819) = 0.0327 \text{ moles} \approx (0.03276 \times 122.063236) \approx 4 \text{ grams}$$

Composition of binder and water are based on the mullite phase in the  $\text{SiO}_2\text{-Al}_2\text{O}_3$  phase diagram. Mullite is the crystalline Aluminum Silicate in the molecular ratio of  $3 \text{ Al}_2\text{O}_3 + 2\text{SiO}_2$ . From the phase diagram, the solid contain percentage of CMC (binder) is equal to 0.4% while water is 37.78%.

### 3.4.2 Impregnation Process

The resulting slurry from the ceramic slurry preparation is then impregnated into cut of the selected Polyurethane foam. This process is called an impregnation process. There are 2 ways that have being determined can be used to impregnate the slurry into the foam which are:

1. Vacuum impregnation technique.
2. Manual compression technique.

In the vacuum impregnation technique, the impregnation is done within a vacuum dessicator (Figure A3) while in the manual compression technique; the impregnation will be done within a beaker by an aid of self-made pusher. Details of both techniques are shown in appendix 3 and 4 respectively.

### 3.4.3 Drying and Calcination Process

After the impregnation process, the combination of foam with the ceramic will undergo drying process to remove the water within it using electrical oven. The drying is executed at a maximum temperature of  $80^\circ\text{C}$  before is left to cold down to room temperature. This will be continue with a calcinations process whereby the organic additives were removed using an electric furnace tool. The dried powder is calcined at a temperature of from about  $700^\circ\text{C}$ . to about  $900^\circ\text{C}$  (Rice, 2003).

### **3.4.4 Sintering/Firing Process**

The next process the slurry preparation will be firing and re-firing correspondingly before the final product is produced. This firing and re-firing process is also known as a sintering process. Reed (1995) in his book states that the firing process involves 3 stages:

1. Organic burnout and elimination of gaseous products of decomposition and oxidation.
2. Sintering
3. Cooling

The sintering process is meant to eliminate the foam in order to produce a microstructure with the required properties. In sintering process, the particles have joined together into an aggregate that has strength. The firing process will be prepared using the electric furnace and will be done with a slow firing rate ( 1° C/minutes ) followed by rapid firing with a rate of 5 to 10° C/minutes.

### **3.4.5 Characterization Process**

The characterization of the resulting foam will be analytically test in terms of its density, porosity, pore structure, pore individual shape, pore size distribution and crushing strength as well as refractoriness. The final product will be tested using universal testing machine to determine the crushing strength, SEM and optical microscope for the texture analysis, and will undergo a high temperature refractoriness testing using hi-temp differential scanning calorimeter, DSC. This characterization process will be done in the second phase of this final year project.

#### **3.4.5.1 Density**

##### **3.4.5.1.1 Bulk density, $\rho_1$**

Bulk density,  $\rho_1$  is measured by using a simple density formula;

$$\rho_1 = m/V \quad (\text{kg/m}^3) \quad (6)$$

Where;  $m$  is mass (kg) and  $V$  is the volume of the sample calculated as;

$$V = t \times w \times l \quad (\text{m}^3) \quad (7)$$

Where;  $t$  is the thickness,  $w$  is the width and  $l$  is the length of the sample as illustrated in figure 5 below.

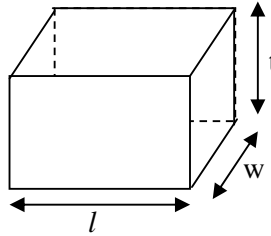


Figure 5: Sample dimension

#### 3.4.5.1.2 Apparent density, $\rho_2$

An apparent density,  $\rho_2$  is measured by submerging the sample into a beaker that consists of distilled water (Figure 6) to measure the displacement of the foam when being submerging in the water.

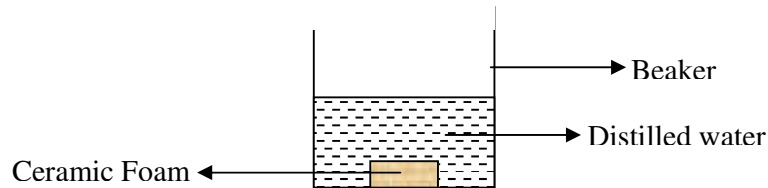


Figure 6: Apparent density method

#### 3.4.5.1.3 True density, $\rho_3$

As illustrated in figure 7, pycnometer is a flask, usually made of glass, with a close-fitting ground glass stopper with a capillary tube through it, subsequently allows air bubbles to escape from the apparatus. This allows the density of a fluid to be measured accurately, by reference to an appropriate working fluid such as water or mercury, using an analytical balance.(Wikipedia, 2008). The methodology of measuring the true density using pycnometer is as follows (Reed, 1995);

1. Empty pycnometer is weighted,  $W_0$
2. The pycnometer with particles is weighted,  $W_1$
3. The pycnometer with particles filled with liquid (Kerosene) is weighted,  $W_2$
4. The pycnometer alone filled with liquid (Kerosene) is weighted,  $W_3$

Then the density of the particles,  $D_p$  can be measured using the following formula;

$$D_p = [ (W_1 - W_0) / \{ (W_3 - W_0) - (W_2 - W_1) \} ] \times (D_L - D_A) + D_A \quad (8)$$

Where  $D_L$  is density of air, and  $D_A$  is density of the liquid (Kerosene).



Figure 7: Pycnometer



## **CHAPTER 4**

### **RESULT AND DISCUSSION**

#### **4.0 RESULT**

The experiments for the first phase of this course are focusing more on the selection of the template from four different types of PU-sponges (appendix 5). The preference of these four types of PU sponge is based on the availability and accessibility on the market. There are two experiments involve in selecting the template which are experiment on determining the characteristic of the PU-sponges using TGA analysis, and experiment on determining the pore structure and composition of the PU-sponges using SEM-EDS machine.

The experiment on determining the optimum composition of the ceramic slurry is executed in order to optimize the final product. With the optimum composition, the firing schedule for the sintering can be constructed. The final product will then go through characterization analysis.

#### **4.1 Template selection**

##### **4.1.1 TGA Analysis**

Four different types of Polyurethane (PU) sponge are to be selected as a template for backbone of the ceramic in producing the refractory ceramic foam. The sponges have differences in term of composition and porosity structure. All four of the sponges were analysed using TGA tool to identify the changes of weight over a range of temperatures of each sample to select the best type of sponge to be the template. The results from the TGA experiment for each samples is displayed in appendix 6 while the overall result is shown in figure 8 in the next page. The result from this experiment is summarized in table 4.

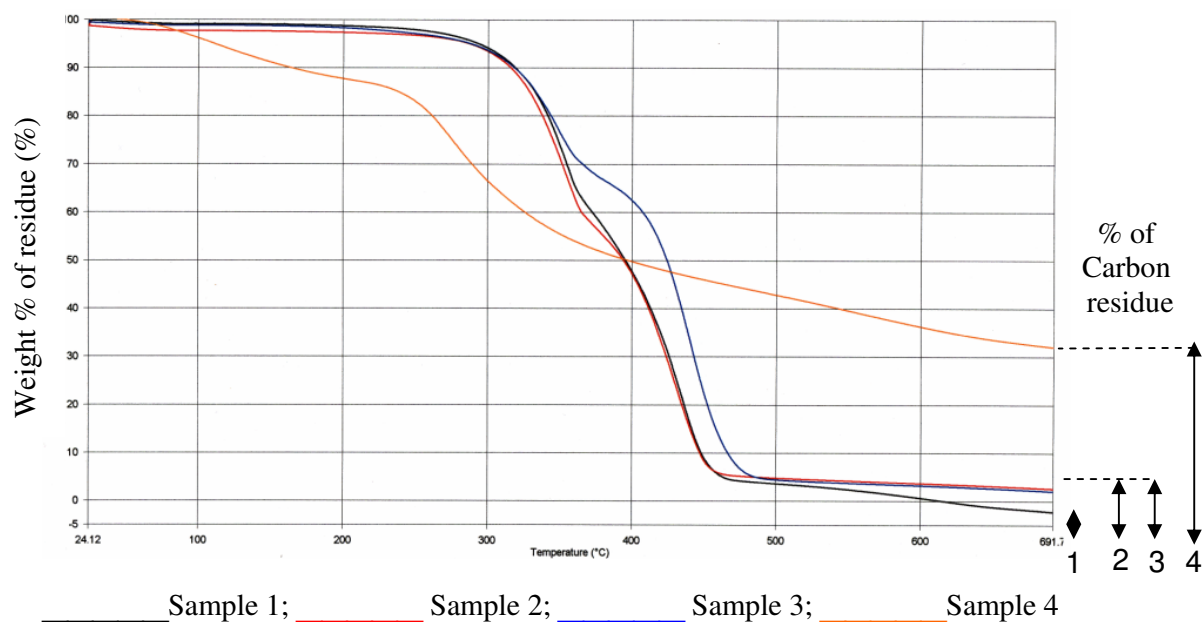


Figure 8: TGA result of all 4 samples

Table 4: TGA analysis result

Sample	Onset Temperature (°C)	Degrading Slope (Weight% / °C)	Carbon residue (%)
1	360	0.6	0.1
2	350	0.6	3
3	380	0.7	2
4	260	0.1	27

#### 4.1.2 SEM-EDS Analysis

The selected sponge is then further analyzed in term of its pore structure and compositions. The result of SEM image of the selected sponge (sample 1) is displayed in figure 9. The images for the other 3 sample are displayed in figure A7a, b and c in appendix 7.

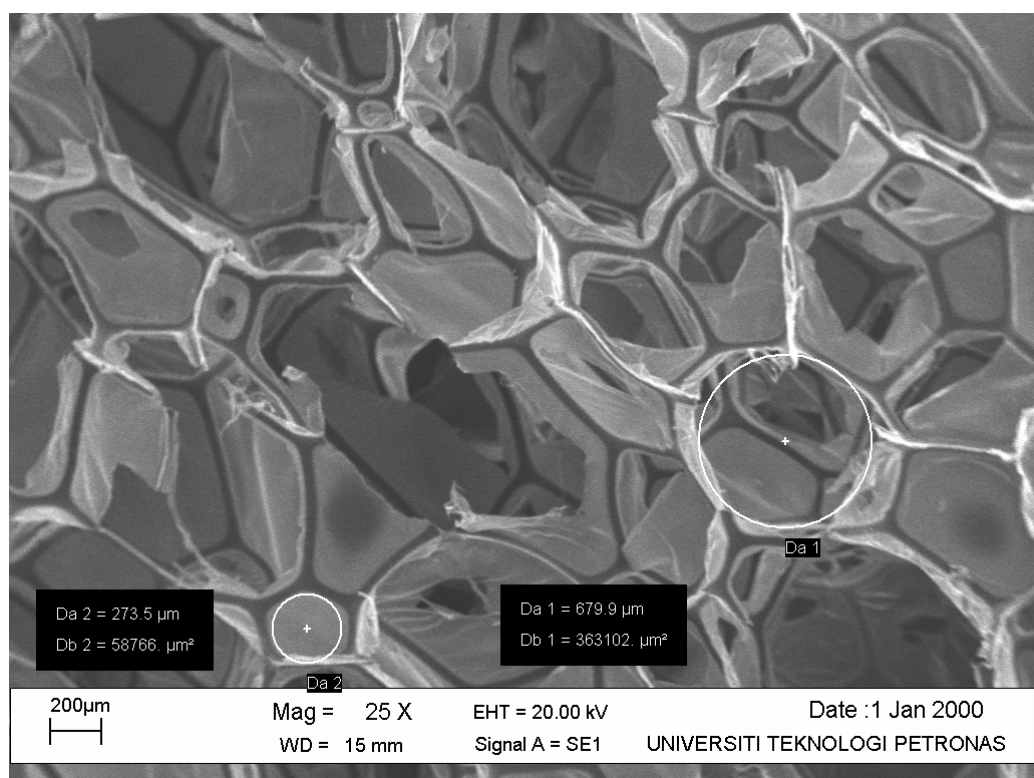


Figure 9: SEM image of PU-foam sample 1

The result of EDS analysis on the composition of each PU-sponges is summarized in table 5 below.

Table 5: Composition of each sample using EDS

Sample	Element	Weight (%)	Atomic (%)
1	Carbon	68.12	74.59
	Oxygen	29.47	24.23
2	Carbon	68.03	73.92
	Oxygen	31.97	26.08
3	Carbon	70.38	75.99
	Oxygen	29.62	24.01
4	Carbon	39.54	49.62
	Oxygen	46.39	43.71
	Magnesium	3.57	2.21
	Chlorine	10.50	4.46

## 4.2 Optimum Composition

The optimum composition is determined by measuring the weight loss of the burnt sample with unburned sample of various percentages of solid contents. For this project, the percentage of solid content that is being considered are at 15%, 45%, 70% and 85%. The result of the difference in weight of each sample with regards to solid content is displayed in figure 10.

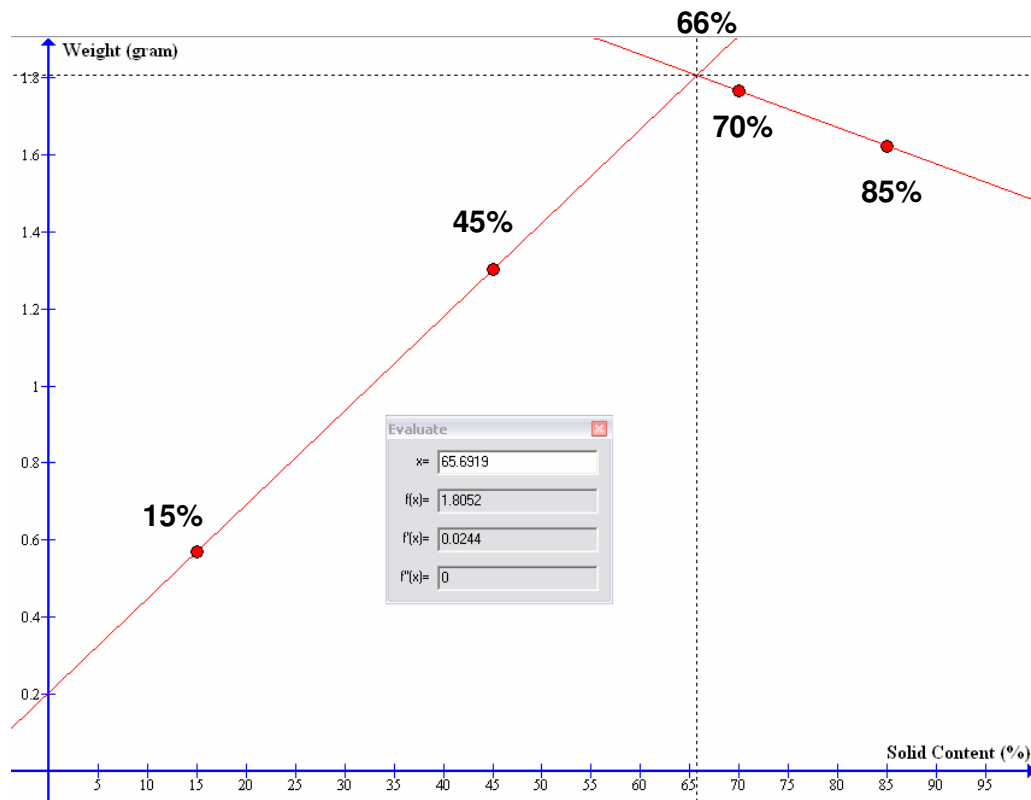


Figure 10: Weight constant volume versus solid contents of ceramic impregnated PU-foam

The graph shows that the optimum composition is at 66% of solid content. Further calculation using the 66% of solid content gives the optimum compositions data in table 6.

Table 6: Optimum composition of 66% solid contain

No	Mass Proposed (g)	A(mole)	SMS (mole)	A(mass,g)	SMS(mass,g)	Total solid mass (g)	Binder (g)	Water (cm <sup>3</sup> )
1	5	0.049	0.041	3	2	5	0.030	2.545
2	10	0.098	0.082	6	4	10	0.061	5.091
3	15	0.147	0.123	9	6	15	0.091	7.636
4	20	0.196	0.164	12	8	20	0.121	10.182
5	25	0.245	0.205	15	10	25	0.152	12.727

### 4.3 Firing Schedule

The firing schedule is constructed based on the TGA curve (figure 11) of the complete mixture of the ceramic slurry with the PU-sponge. The TGA is done to the fully dried sample to estimate the solid degradation in weight of the sample with increasing temperature.

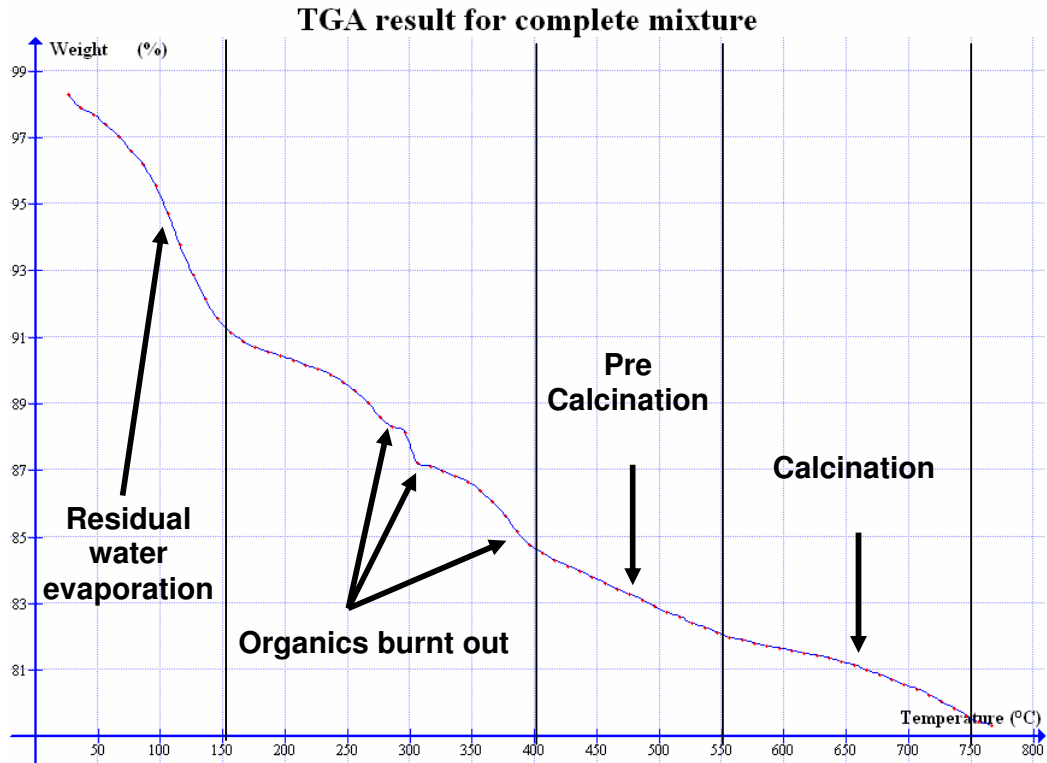


Figure 11: TGA curve for the complete mixture

Assumption has to be made to the dwell range for the highest sintering temperature to be executed at a highest temperature of 1000°C as the available furnace can only be used up to a maximum of 1100°C. In doing so, estimation is made using 235950/(T-27) graph (figure 12) which is fully developed based on the value of practiced dwell time of the solid Alumina sintering (  $t_{\text{dwell@1600}^{\circ}\text{C}} = 2 \text{ hours } 30 \text{ minutes}$ ) as figured out in the practiced firing scheduled graph (figure A8) in appendix 8 where it is practicable for estimation to be made as the graph is exponentially trim down of time over the temperature.

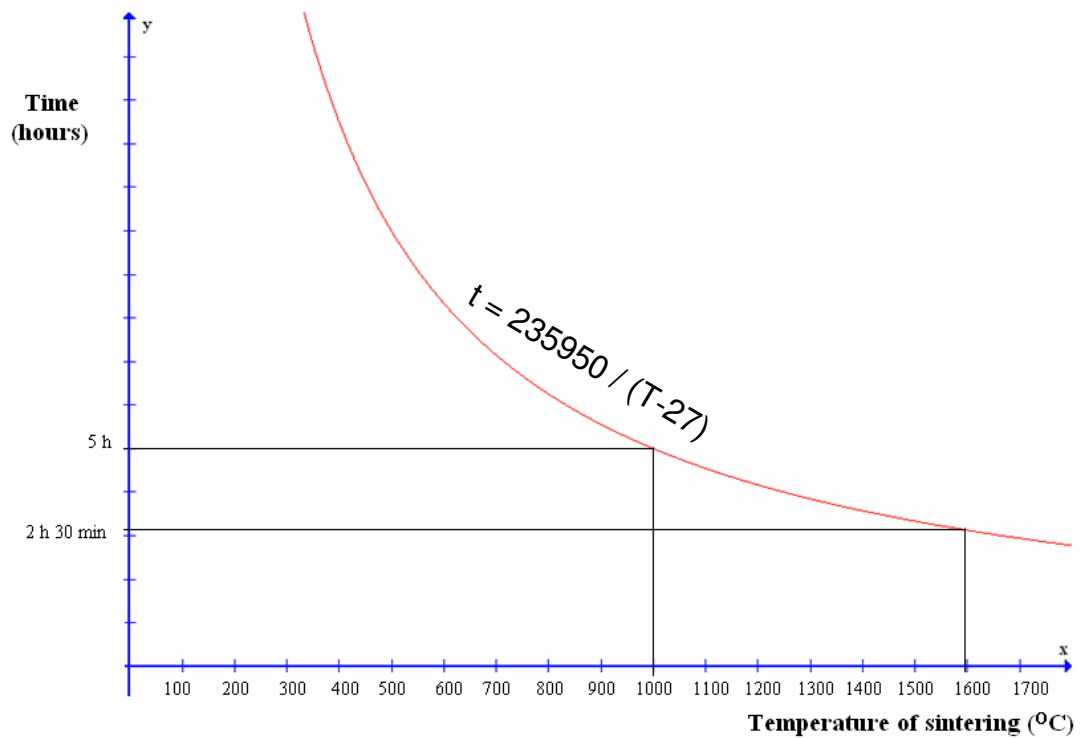


Figure 12: Dwell range estimation at the peak sintering temperature.

By estimation using 235950/(T-27) graph, total dwell time (in hour) of sintering using maximum temperature of 1600 °C is equal to 2 hours 30 minutes (appendix 8). From the graph above, the total time of sintering using highest temperature of 1000 °C is equal to approximately 5 hours.

$T_{\text{new}} = 235950 / (T_{\text{old}} - 27)$  , as  $T_{\text{old}} = 814$ ,  $T_{\text{new}} = 235950 / (814 - 27) = 298.6$  minutes  $\approx 5$  hours. Room temperature taken is  $= 27^{\circ}\text{C}$

Based on the TGA graph of the complete mixture of ceramic slurry with the PU-sponge and the  $235950 / (T - 27)$  estimation graph, the overall firing schedule as depicted in figure 13 is constructed.

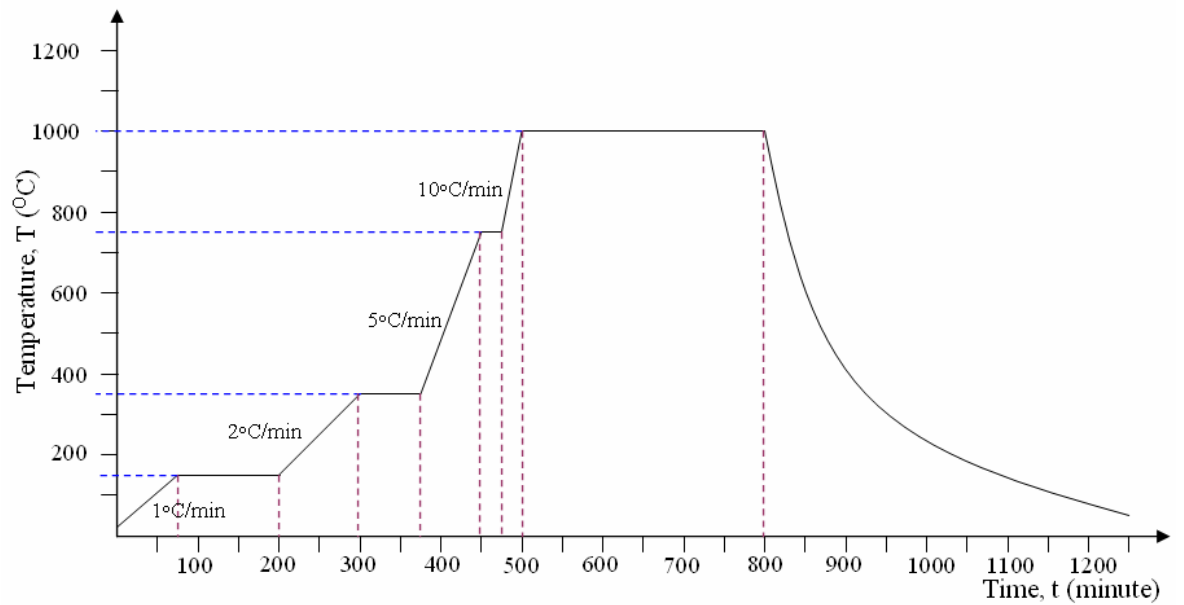


Figure 13: Overall firing schedule

#### 4.4 Sintering

The sintering is executed using a (20x10x10) mm sample as depicted in figure 14 a.

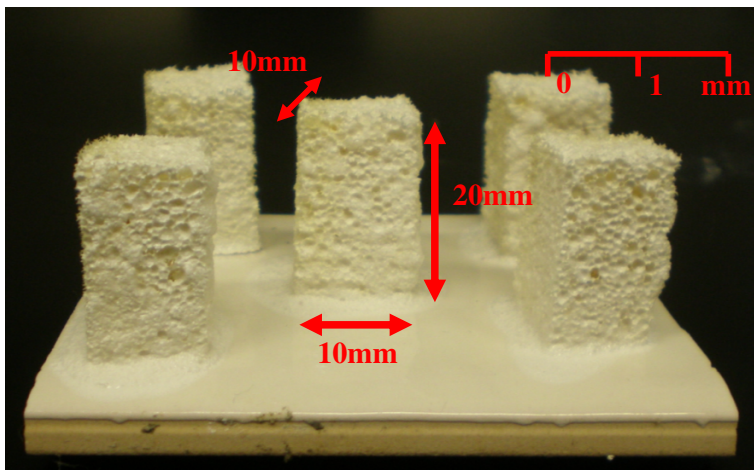


Figure 14 a: Sample before sintering

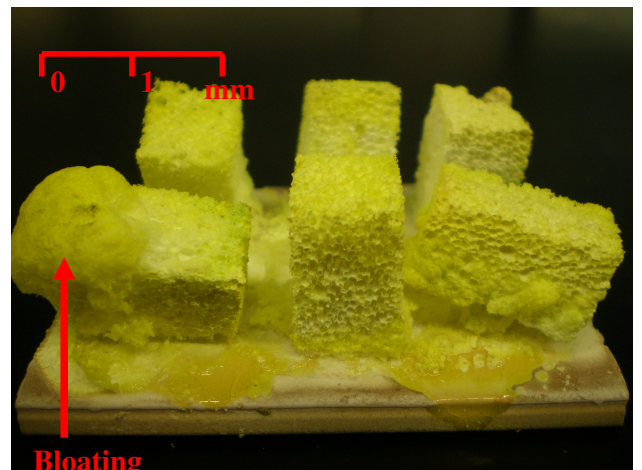


Figure 14 b: Sample after sintering

The sample is sintered on a piece of tile to avoid any contamination with the furnace floor which might be contaminated with foreign substances and such a way that a small amount of Alumina powder is layered between the sample and the tile to avoid the sample from sticking to the tile after sintering. Both visual images of the sintered ceramic foam before and after sintering are depicted in figure 14 a, and b respectively.

## 4.5 Characteristic

### 4.5.1 Microscopic analysis

The sintered ceramic foam is analyzed microscopically using SEM. The microscopic picture of the ceramic foam is shown in figure 15.

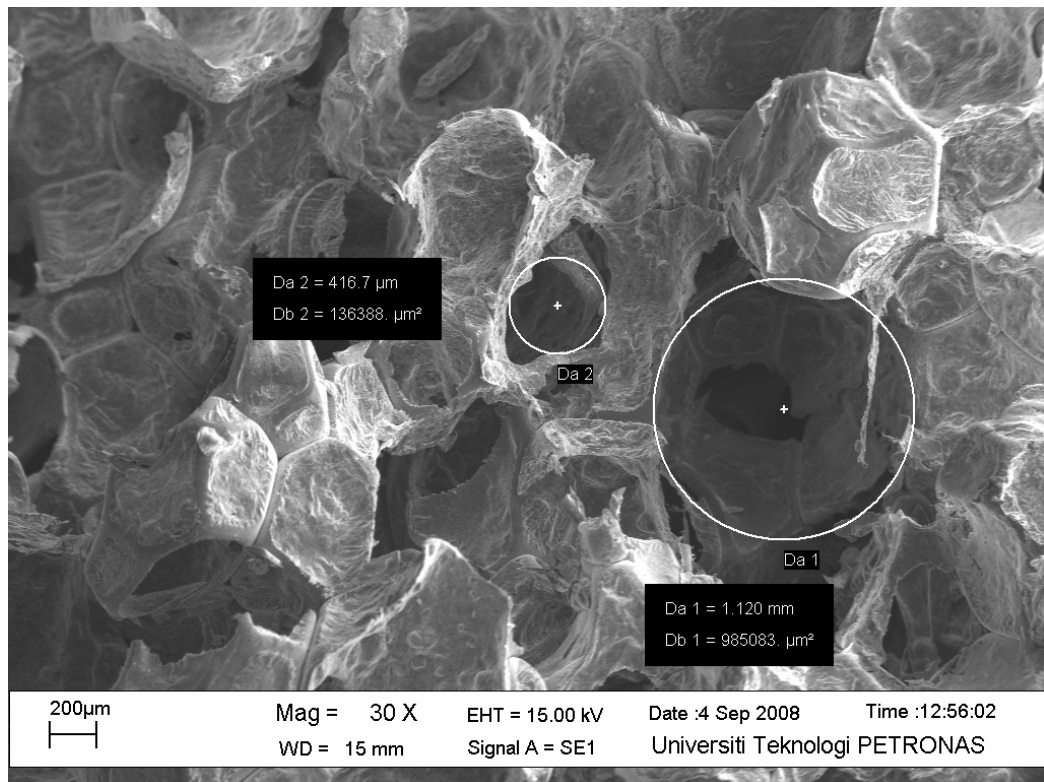


Figure 15: SEM image of fired ceramic foam



From the image of figure 15, it is clearly observed that the ceramic particle is well sintered according to the PU-sponge shape. The principle behind this is explained with the schematics in figure 16 below.

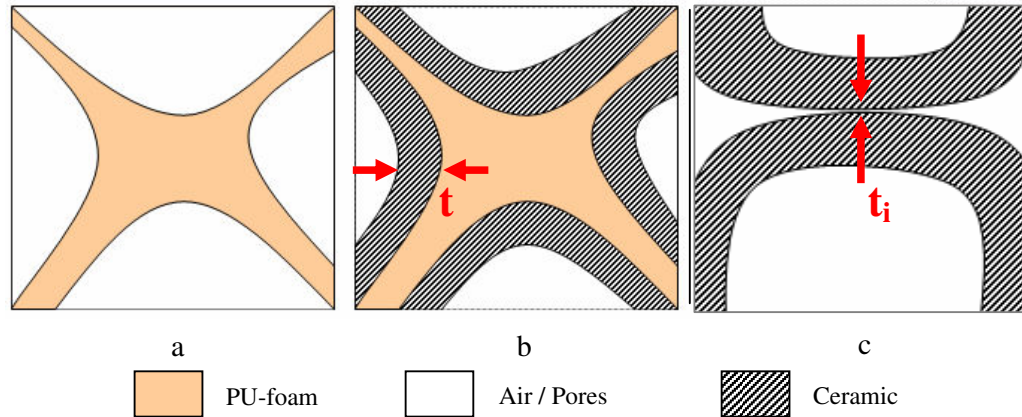


Figure 16: Schematic of forming mechanism of ceramic foam

Figure 16a illustrated the pores and wall of the PU-sponge. While figure 16b shown the impregnated ceramic slurry into the PU-sponge. The thickness ( $t$ ) of the ceramic slurry that is stacked on the PU-sponge wall is highly depending on two main variables that is:

1. Viscosity of the ceramic slurry.
2. The rheology of the ceramic slurry which is depending on the ingredients that makes up the ceramic slurry as well as the composition of each of the ingredients.

Figure 16c shown the final product of the ceramic foam which as can be seen the PU-sponges is no longer exist in the system as it was burnt out during the sintering process. As can be noted, the air interference gap will replace the PU-sponge. Some of the gap is thin and known as the sintered intercellular interference,  $t_i$ .

The chemical composition of the final product is analyzed using EDS. The chemical components of it is depicted in figure 17 and presented in table 7.

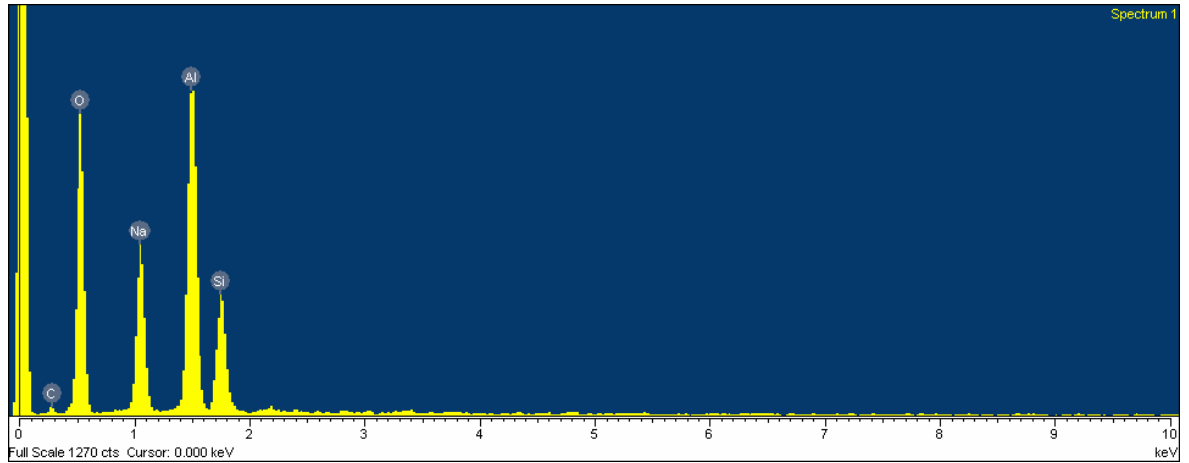


Figure 17: EDS spectrum of the final fired product of ceramic foam

Table 7: Chemical composition of the final product

Element	Weight (%)	Atomic (%)
Carbon	5.39	8.33
Oxygen	52.95	61.43
Aluminium	18.59	12.79
Sodium	15.05	12.15
Silicon	8.03	5.30

#### 4.5.2 Pore linear density

From the SEM image of the ceramic foam, the pore linear density in a unit of pores per unit inch (PPI) can be calculated. The calculation is made in average.

$$[1600\mu\text{m}/5 \text{ pores}] \times [1\text{m}/\mu\text{m}] \times [1 \text{ inch}/ 0.0254\text{m}] \approx 80 \text{ pores/ inch}$$

#### 4.5.3 Density

##### 4.5.3.1 Bulk density, $\rho_1$

Average using equation 6 and 7 in page 21, the bulk density of the final product is calculated as follow;

$$\text{Weight of sample}_{\text{average}}, m = 1.704 \text{ g}$$

Using equation 7, the volume of sample,  $V = (2 \times 1 \times 1) \text{ cm}^3 = 2 \text{ cm}^3$

Hence the bulk density using equation 6,  $\rho_1 = m/V = 1.704 \text{ g} / 2 \text{ cm}^3 = 0.852 \text{ g/cm}^3$

$$\therefore \rho_1 \approx 0.852 \text{ g/cm}^3$$

#### **4.5.3.2 Apparent density, $\rho_2$**

The apparent density,  $\rho_2$  is determined experimentally. The data and calculation for the experiment are as follow;

- Weight: Beaker = 97.641 g ;
- Water (100 ml) + beaker = 201.268 g ;
- Water + beaker + ceramic foam = 203.3 g.

So the ceramic foam mass,  $m = (203.3 - 201.3) \text{ g} = 2 \text{ g}$ .

Hence the apparent density using equation 6,  $\rho_2 = m/V$  as  $V = 2 \text{ cm}^3$ ;

$$\therefore \rho_2 = (2 / 2) \text{ g/cm}^3 \approx 1 \text{ g/cm}^3$$

#### **4.5.3.3 True density, $\rho_3$**

From the steps given in section 3.4.5.1.3 of the true density using pycnometer and applying the equation 8, the true density,  $\rho_3$  obtained is  $1.241 \text{ g/cm}^3$ .

#### **4.5.4 Product shrinkage**

Product shrinkage is a very important measurement in ceramic production as the final product of the ceramic will not be the same dimension with the sample input. The sample will shrink as the PU-foam will be burnt out leaving a sintered air interference gap. Hence the design should be in such away that the input must be slightly higher than the desired output by plus the shrinkage dimension.

##### **4.5.4.1 Linear shrinkage**

Linear shrinkage is determined for each dimension of the sample i.e for it length, width and its thickness by comparing final dimension with the original dimension. The linear shrinkage calculation is given by;

Linear shrinkage =  $([l_o - l] / l_o) \times 100\%$  ;  $([w_o - w] / w_o) \times 100\%$ ;  $([t_o - t] / t_o) \times 100\%$

Data:  $l_o = 20$  mm;  $w_o = 10$ mm and  $t_o = 10$ mm ;  $l = 18.6$ mm;  $w = 8.4$ mm;  $t = 8.7$  mm.

Hence; linear shrinkage= Length,  $l = ([20 - 18.6] / 20) \times 100\% = 7\%$ ; width,  $w = ([10 - 8.4] / 10) \times 100\% = 16\%$ ; thickness,  $t = ([10 - 8.7] / 10) \times 100\% = 13\%$ .

#### 4.5.4.2 Bulk volume shrinkage

Bulk volume shrinkage is determined by comparing the volume of the original sample,  $V_o$  with the final product volume,  $V$ .

$$V_o = (20 \times 10 \times 10) \text{ mm}^3 = 2000 \text{ mm}^3 ;$$

$$V = (18.6 \times 8.4 \times 8.7) \text{ mm}^3 = 1359.288 \text{ mm}^3$$

Hence the bulk volume shrinkage =  $([V_o - V] / V_o) = ([2000 - 1359.288] / 2000) \text{ mm}^3$   
 $= 0.320 \text{ mm}^3$  or 32%.

#### 4.5.5 Crystalline analysis

The final product is tested in term of its crystallinity. Crisrallinity analysis is very important to determine whether the final product is well crystallized as crytallinity determines the refractoriness of the final product. Apart from that, the crystallinity which is done by using XRD is also meant to identify the final materials that develop the final product. From the test, it is found that the crystal structure of the final product is an Orthorhombic crystal structure and the materials that develop the final product is found to be Sodium Aluminum Silicate. The result obtained from XRD test is shown in figure 18.

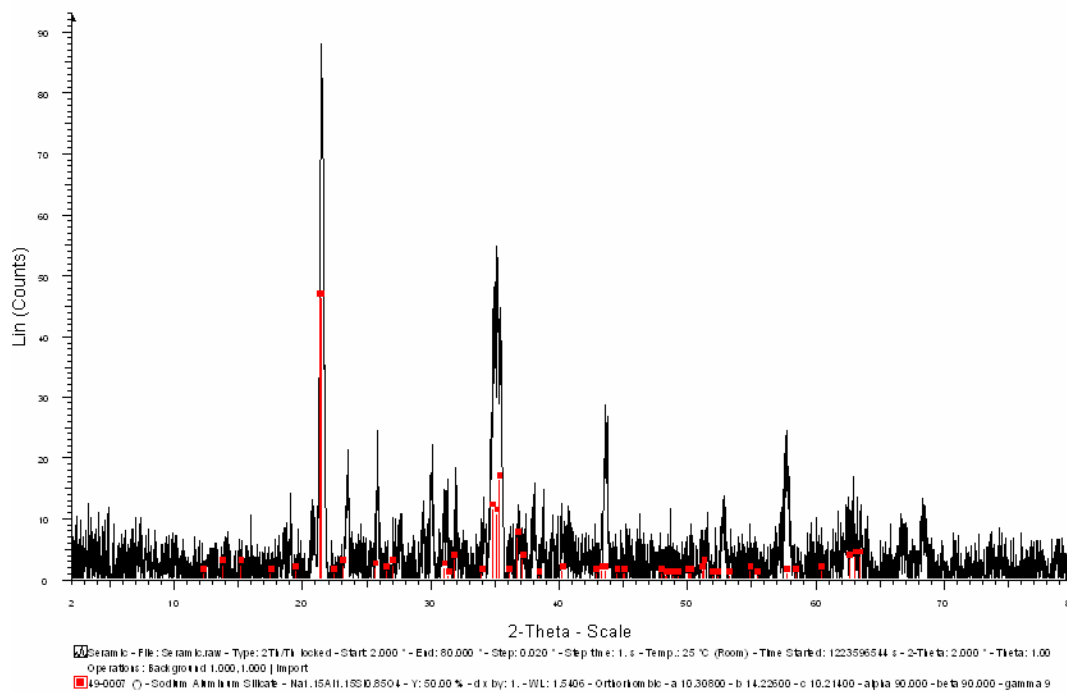


Figure 18 : Crystallinity analysis using XRD

#### 4.5.6 Crushing strength

The final product is also tested in term of its crushing strength. The mechanical testing machine is used to test the final product by a compression technique. The test was done with a load speed of 10mm per minutes with a maximum load of 3000 N. The resulted stress versus strain curve is depicted in figure 19.

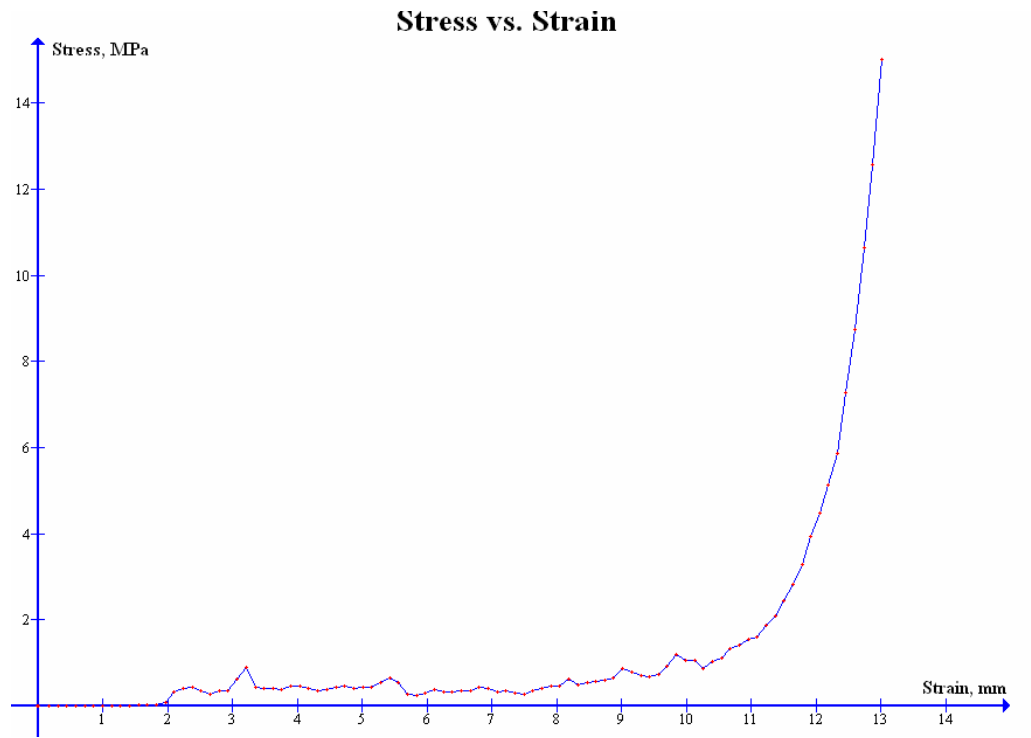


Figure 19: Stress vs strain graph for the final fired product of ceramic foam

Crush strength<sub>foam</sub> is equal to the stress at which continuous plastic collapse begins which is from the graph the  $\sigma_{pl}$  start to occur at  $\sigma = 2.236932$  MPa of  $\varepsilon = 0.407643$  mm. This resulted for the final product to be able to sustain up to 7 kg of load before it fractures.

#### 4.6 Discussion

From the TGA results, sample 1 has the least percentage of carbon residue compared to the other samples. The carbon residue is the main criteria in making decision on which type of sponge to be used as the template. The least contains of carbon residue is most preferable as the carbon will react with the other substance such as the processing additives in the sintering process further on. This reaction will affect the final product chemically. Apart from that, the carbon contain also can affect the heating schedule of the ceramic foam as it will enlarge the schedule for elimination

of the carbon to occur. The remaining carbon particles in the final product will affect the product strength as it can initiate a crack to occur as they created holes within the product which at certain time will enlarge and combined with other holes to initiate a crack to happen hence damaged the product. Hence, sample 1 with least carbon residue is chosen to be the template.

From the SEM analysis, the pore structure of the sample 1 is more uniform compared to the others sample. It also has a small size of pore wall contrasted with others sample which is effective in the firing process which it can reduce the chances of collapse of the ceramic structure when the template is removed away during the sintering process. The EDS analysis is important to identify the components that built up the PU-sponge. Result shows that all samples consist of 2 main elements which are Carbon and Oxygen. Sample 3 have the largest amount of weight percent of Carbon contains while sample 4 has the least. Both sample 1 and 2 consist of a medium weight percentage of Carbon contains. This display the effectiveness of the sample 1 compared to the others tested samples.

In order to structure a good process flow of making the ceramic foam, the optimum composition is determined. This optimum composition can optimize the final product apart of can cut off the number of experiments (if using try and error method) as it reduces the number of variables that need to be controlled during the sintering process.

The firing schedule is determining by using experimental procedure using TGA analysis as well as using estimation based on practiced work that have been done through the literature review and collaboration with a researcher. The estimation is done to suit the sintering process with the equipment available hence if there is equipment that can provide up to 1600°C of maximum temperature, the estimation part can be ignored. In this project the sintering is done in two different phase as to for more efficient sintering process as well as to suit with the working hour of the technician in charge of the equipment. The first phase is to sinter the sample from room temperature up to 750°C before continue with the second phase from room temperature to 1000°C.

The chemical contents of the final product yet appear to have Sodium and Silicate element by which theoretically the Sodium Silicate (processing additive) supposedly will be burnt out entirely during the sintering process. However by using XRD analysis, it is shown that the remaining Sodium and Silicate is behaving their own characteristic not in term of a single Sodium Silicate characteristic anymore. This is also proved when the final product is not absorbing water particles (as the Sodium Silicate is acting as a hydrate element) when exposed to the air as likely to happen before it gets sintered. Hence the existence of the Sodium and Silicate is not affecting the characteristic of the final product.

The final product in this project as depicted in figure 14 b seems to be changing in colour (from white to yellow). This as a result of a contamination of the sample with the furnace's surface which having a transition type of material waste still sticking on the furnace's surface as it gives a yellow like colour to the final product. The contamination has being assumed not to affect the final product characteristic. Nevertheless, further experiment using different furnace give a positive result (no colour changes) revealed that the effect of colour changed is due to the contamination affect not from the ceramic foam materials itself.

In addition, the compositions of the final product also still having Carbon particles (5.39 weights %) i.e the Carbon is not being fully eliminated in the sintering process, nonetheless the percentage of the Carbon comparing with the initial weight % inside the PU-sponge (68.12 weights %) is a decreasing about 85 % in weight %. This shows that the effect of Carbon is reduce in the final fired product.

The true density,  $\rho_3$  is appears to be larger than both the apparent,  $\rho_2$  and the bulk density,  $\rho_1$  where it can be summarized as  $\rho_3 > \rho_2 > \rho_1$ . This illustrates the effective and accuracy of the apparent density method in calculating the density of the ceramic foam as the ceramic foam is a complex pore shaped material.

The cristallinity of the product is tested in order to measure whether it is well crystallize or not as cristallized product of ceramic foam is more suitable to be used in many applications especially as a refractory material. Using the XRD tool the



crystal structure of the final product found to be an Orthorhombic crystal structure and the materials that develop the final product is found to be Sodium Aluminum Silicate. From this analysis also the materials building the final product is analyzed as compared to the materials before it is fully fired. This is important to ensure that the ceramic material acts independently with its own characteristics with no disturbance from other processing additives which theoretically is eliminated during the sintering process.

The final product is also being tested in its crushing strength which is aimed to determine the physical strength of the final product. The result shows that the final product can sustain up to 7 kg of weight where  $\sigma_{pl}$  start to occur at  $\sigma = 2.236932$  MPa of  $\varepsilon = 0.407643$  mm before it fractures.

## CHAPTER 5

### CONCLUSION AND RECOMMENDATION

#### 5.0 CONCLUSION AND RECOMMENDATION

##### 5.1 Summary/Conclusion

Throughout the research from the past paper works and experiments conducted in the project, it is found that the refractory ceramic foam can be processed economically via powder routes of Alumina, by an aid of Polyurethane sponge as template. This will occurs with the present of processing additives such as Carboxyl Methyl Cellulose (CMC) as binding additives, Sodium Meta Silicate (SMS) as a sintering aid and distilled water as a wetting agent. The flow of the process is summarized in figure 4 (section 3.1). Ceramic and other additive materials are judiciously characterized to control the final product. All the analyses and techniques selected are wisely planned so that those characteristics that are determined give the essential data with the best result.

Sample 1 from four different type of PU-sponge is selected as the templates as it has the least percentage of carbon contains, most uniform pore structure and a medium amount of carbon contains compared to the other samples. The optimum composition of materials for this project is determined to be at 66% of solid contents. This composition is used as the final composition of the ceramic slurry to be impregnated into the cut of selected PU-sponge and further on to undergo a sintering process to eliminate the PU-sponge and other processing additives.

The characteristics of the final product of the ceramic foam are listed as follow;

- |  |  |
|--|--|
| 1. PPI (pores per inch) = 80 ppi.                        | 6. Bulk volume shrinkage = 0.320 mm <sup>3</sup> . |
| 2. Bulk density, $\rho_1 \approx 0.852 \text{ g/cm}^3$ . | 7. Crystall structure: Orthorhombic.               |
| 3. Apparent density, $\rho_2 \approx 1 \text{ g/cm}^3$ . | 8. Product material: Sodium Aluminum               |
| 4. True density, $\rho_3 \approx 1.241 \text{ g/cm}^3$ . | Silicate.  |

5. Linear shrinkage;  $l = 0.07$  mm;  
 $w = 0.16$  mm;  $t = 0.13$  mm.

9. Crush strength $_{\text{foam}} = 2.236932$  MPa.  
Load $_{\text{maximum}} = 7$  kg

## 5.2 Recommendation

Thorough out the project, the writer has comes out with some recommendations for the improvement of the project as well as for further consideration that related to the project.

1. The method/technique of impregnating the ceramic slurry into the cut of PU-sponge can be enhanced. It may be done with the vacuum dessicator technique or other techniques that may be invented in the future. The manual compression method which is used by the writer in this project can be improved in the future by developing an automatic compression tool for a easier and faster ways in infiltration process or if there is a need for a mass production of it.
2. As the project is more concern in producing small scale of ceramic foam products, the application may vary among the small scale products only such as bone substitution and others. Further study in the future might consider production in large scale or large size of products for more diverse range of applications such as refractory material for furnace, hot gas filter and others.
3. Apart from that, the characteristic of the final product also need to be tested in term of its sustainability of heat by using tool like TEM or DTA in order to determine whether it can be used as a refractory material or not which the writer is unable to test it due to unavailability of tool.

## REFERENCES

### **BOOKS**

1. Barsoum, MW. (2003). *Fundamentals of Ceramics*.  
United Kingdom: IOP Publishing Ltd.
2. Gibson, L. J. & Ashby, M.F. (1999). *Cellular solids, Structures and Properties*.  
(2nd Edition). Cambridge, Cambridge University Press.
3. Gum, Wilson; Riese, Wolfram; Ulrich & Henri (1992). *Reaction Polymers*.  
New York: Oxford University Press.
4. Rahaman, M.N. (2003). *Ceramic Processing And Sintering*.  
New York: Marcel Dekker.
5. Reed, J. S. (1995). *Principles of ceramics processing*. (Second edition).  
New York: Wiley.
6. Rice, R.W. (2003). *Ceramic Fabrication Technology*.  
New York: Marcel Dekker.

### **ARTICLES**

1. Andrews, E.W; Gibson, L.J & Ashby, M.F. (1999), *Overview no. 132: the creep of cellular solids*, Acta Mater. 47 [10], 2853.
2. Almiralla, A; Larrecqa, G; Delgado, J.A; Martinez, S; Ginebra, J.A.M.P.(2004),  
*Fabrication of low temperature macroporous hydroxyapatite scaffolds by foaming and hydrolysis of an  $\alpha$ -TCP paste*, Biomaterials 25, 3671.
3. Bagwell, R.B & Messing, G.L. (1996). *Critical factors in the production of sol-gel derived porous Alumina*, Key Engineering Materials vol.115 pp. 44-64.
4. Colombo, P & Modesti, M. (1999) J. Am. Ceram. Soc. 82 573.
5. Fend, T; R. and P. Paal, Reutter, O; Bauer, J & Hoffschmidt, B. (2004), *Two novel high- porosity materials as volumetric receivers for concentrated solar radiation*, Solar Energy Materials & Solar Cells, 84, 291–304.
6. Fitzgerald, T.J & Mortensen, A. (1995), *Processing of microcellular sic foams .1. Curing kinetics of polycarbosilane in air*, J. Mater Sci 30 (4) , 1025.

7. Fitzgerald, T.J; Michaud, V.J & Mortensen, A. (1995), *Processing of microcellular sic foams* 2. Ceramic foam production, J. Mater Sci 30 (4) 1037.
8. Goretta, K.C; Brezny, R; Dam, C.Q; Green, D.J; DE Arellano-Lopez, A.R & Dominguez-Rodriguez, A. (1990), *High Temperature Mechanical Behavior of Porous Open-cell Al2O3*, Materials Science and Engineering, A 124, 151
9. Hutmacher, D.W. (2000). *Scaffolds in tissue engineering bone and cartilage*, Biomaterials 21, 2529.
10. Haugen, H; Will, J; Kohler, A; Hopfner, U; Aigner, J. (2004), *Ceramic TiO2-foams: characteri sation of a potential scaffold*, J. Eur.Ceram. Soc. 24, 661.
11. Inui, T; Otawa,T. (1985), *Catalytic combustion of benzene-soot captured on ceramic foam matrix*, Applied Catalysis, 14, 83.
12. Lammers, F.A; De Goey, L.P.H. (2003), *A numerical study of flash back of laminar premixed flames in ceramic-foam surface burners*, Combustion and Flame 133, 47.
13. Maiti, S.K; Ashby, M.F; Gibson, L.J. (1984), *Fracture Toughness of Brittle Cellular Solids*, Sript. Metall. 18, 213.
14. Montanaro, L. ( 1999), *Durability of ceramic filters in the presence of some Diesel soot oxidation additives*, Ceramics International 25, 437.
15. Montanaro, L; Jorand, Y; Fantozzi, G; Negro, A. (1998), *Ceramic foams by Powder processing*, J. Eur. Ceram. Soc. 18, 1339 .
16. Muir, J.F; Hogan, R.E; Jr Skycypec, R.D; Buck, R. (1993), *The CAESAR project*, Sandia Report, SAND92- 2131.
17. Nangrejo, M.R; Bao, X; Edirisinghe, M.J. (2001), *Silicon carbide-titanium carbide composite foams produced using a polymeric precursor*: International Journal of Inorganic Materials 3, 37
18. Nangrejo, M.R & Edirisinghe, M.J. (2002), *Porosity and Strength of Silicon Carbide Foams Prepared Using Preceramic Polymers*, Journal of Porous Materials 9, 131.
19. Qian, J.M; Wang, J.P; Qiao, G.J; Jin, Z.H. (2004), *Preparation of porous SiC ceramic with a woodlike microstructure by sol-gel and carbothermal reduction processing*, J Euro Ceram Soc 24, 3251.

20. Richardson, J.T; Peng, Y; Remue, D. (2000), *Properties of ceramic foam Catalyst supports: pressure drop*, Applied Catalysis A: General 204,19–32.
21. Russo, P; Ciambelli, P; Palma, V; Vaccaro, S. (2003), *Simultaneous filtration And catalytic oxidation of carbonaceous particulates*, Topics in Catalysis 22, Nos. 1-2, 123
22. Saggio-Woyansky, Acorr, C.S & Minnear, W.P. (1992), *Processing of porous ceramics*, Am. Ceram. Soc. Bul. 71, 1674 .
23. Schwartzwalder, K & Soners, A.V. (May,21,1963), *Method of making porous ceramic articles*, US 3.090,094.
24. Sepulveda, P & Binner, J.G.P. (1999). *Processing of Cellular Ceramics by Foaming and in situ Polymerisation of Organic Monomers*: J. Eur. Ceram. Soc. 19, 2059
25. Sherman, A.J; Tuffias, R.H & Kaplan, R.B. (1991), *Refractory Ceramic Foams: A Novel High- Temperature Structure*, Am. Ceram. Soc. Bull., 70 [6]1025-29.
26. Sunderman, E & Viedt, J. (1973), *Method of manufacturing ceramic foam bodies*. US Pat no. US Pat no. 3 745 201.
27. Zeschky, J; Goetz-Neunhoeffler, F; Neubauer, J; Jason Lo, S.H; Kummer, B; Scheffler, M; Greil, P. (2003), *Pre ceramic polymer derived cellular ceramics*, Composites Science and Technology 63, 2361.

## **INTERNETS**

1. Marubeni Specialty Chemicals. (2008). *Carboxymethyl Cellulose* . Retrieved February 14, 2008, from <http://www.msi-us.net/productfamily.cfm?id=5>
2. Wikipedia. (2008). *Ceramic Materials* . Retrieved February 11, 2008, from <http://en.wikipedia.org/wiki/Ceramic>

## **APPENDICES**

## Appendix 1: Project Gantt chart

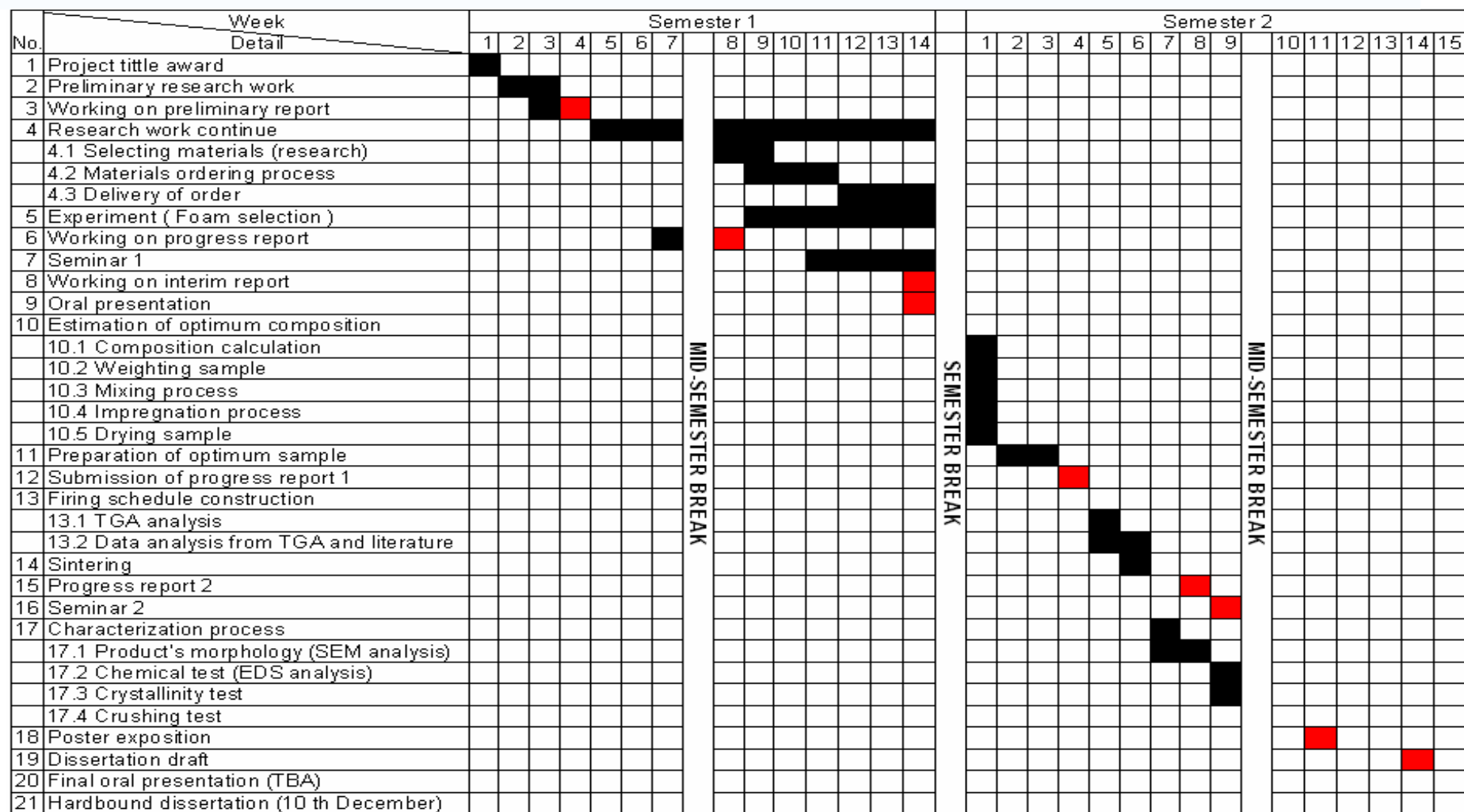


Figure A1: Project Gantt chart



## Appendix 2: Process flow for foaming technique

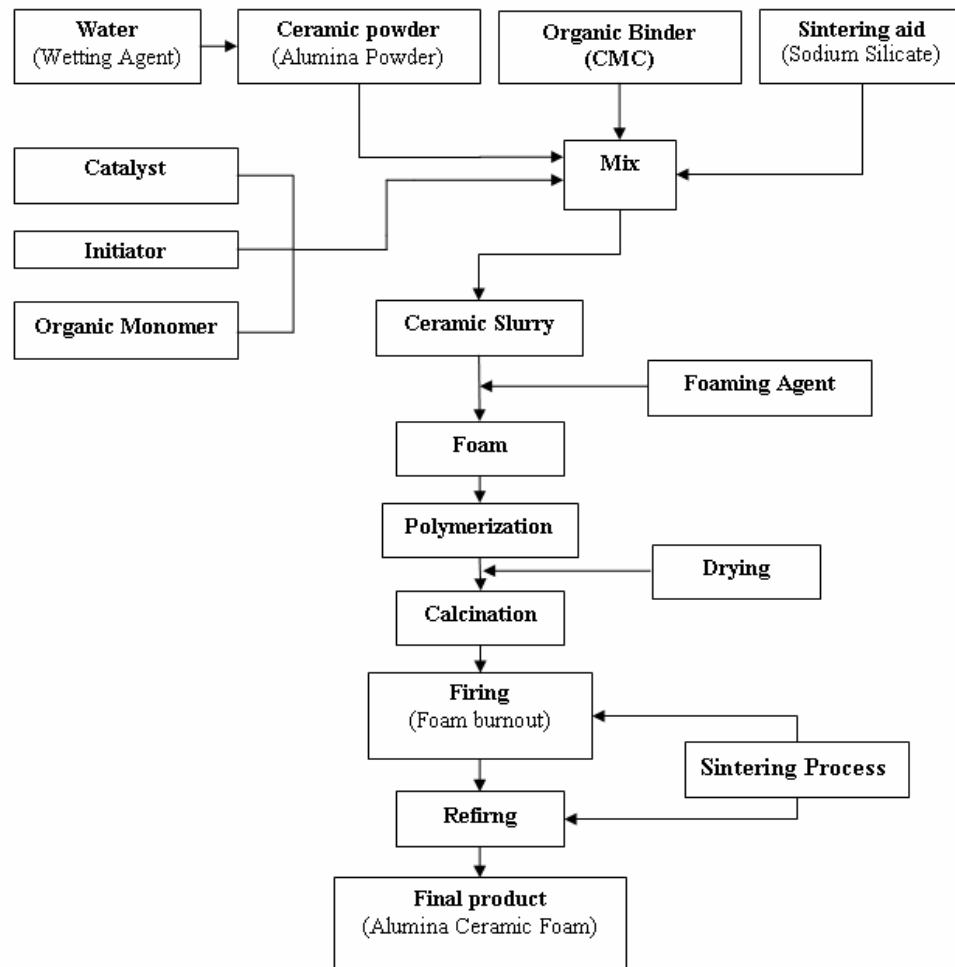


Figure A2: Process flow for Foaming technique

### Appendix 3: Vacuum impregnation technique for impregnation process.

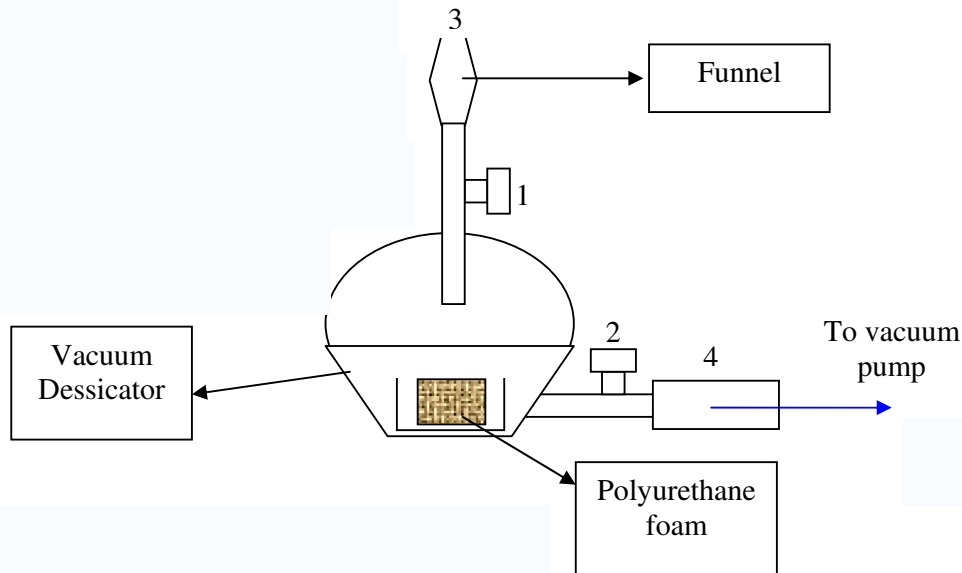


Figure A3: Mechanism of vacuum impregnation technique

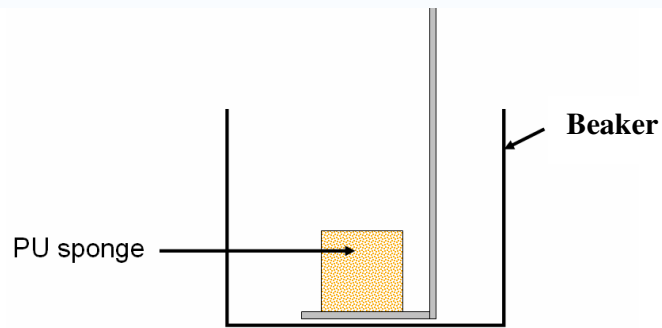
Procedure of vacuum impregnation technique:

1. Vacuum pump is set to on when opening 2 is opened while opening 1 is closed.
2. Opening 2 is then closed.
3. Ceramic slurry is added into 3 (funnel).
4. Opening 1 is opened slowly letting the slurry submerge the Polyurethane foam.
5. Opening 1 is then closed.
6. 4(tube connecting to vacuum pump) is pulled-out.
7. Opening 2 is opened quickly.
8. Impregnated ceramic foam is then slowly taken out.

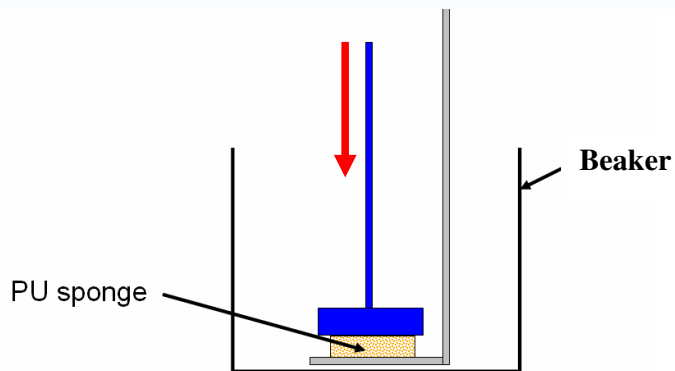
#### **Appendix 4: Manual compression technique for impregnation process.**

Procedure of manual compression technique:

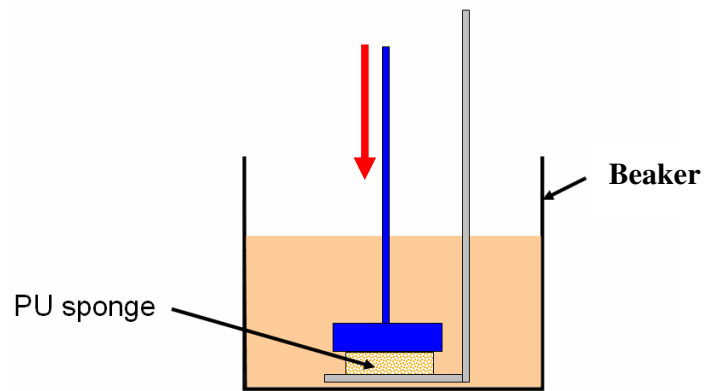
1. The cut Polyurethane sponge is putted into a beaker by using a holder.



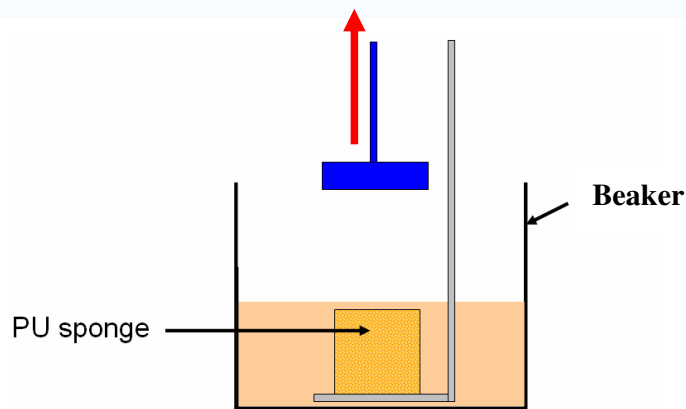
2. Polyurethane sponge is push/compressed.



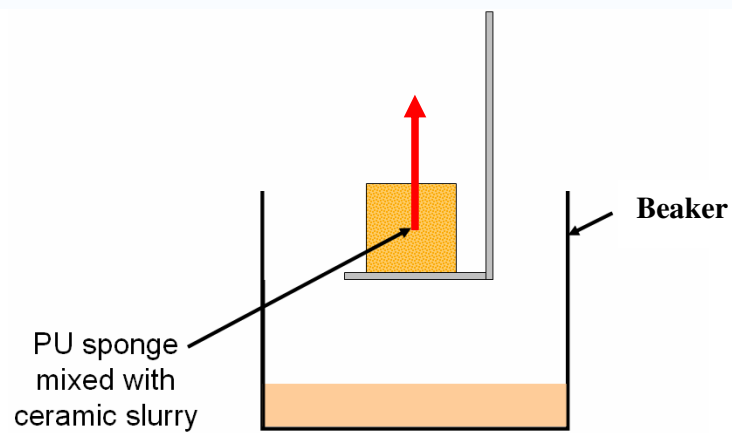
3. Ceramic slurry is poured into the beaker while compressing the PU-sponge.



4. The compression is released at medium speed to ensure the foam can absorb maximum amount of ceramic slurry.



5. The impregnated ceramic foam is slowly taken out.

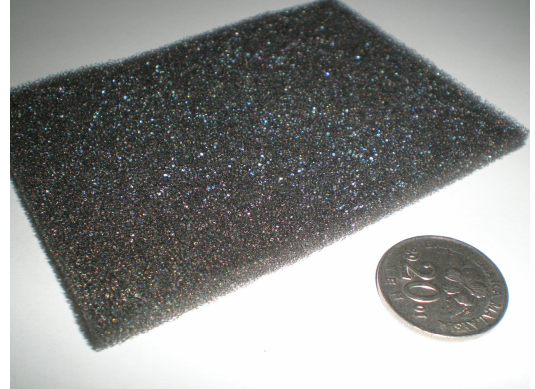


## Appendix 5: Four different types of available PU sponge

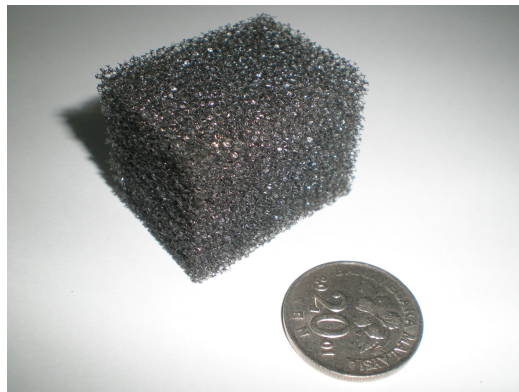
Four different types of available PU sponge that have been consider throughout this project:



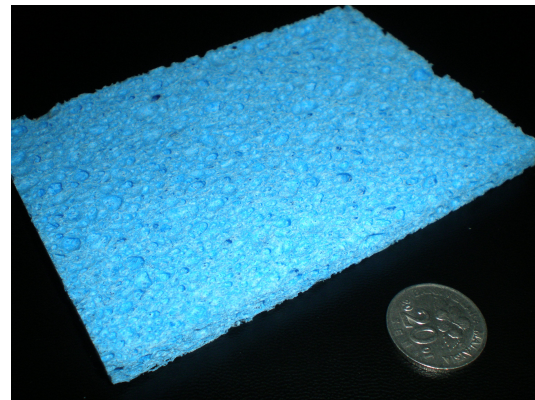
PU-foam sample 1



PU-foam sample 2



PU-foam sample 3



PU-foam sample 4

Appendix 6: TGA result for each sample of PU sponges.

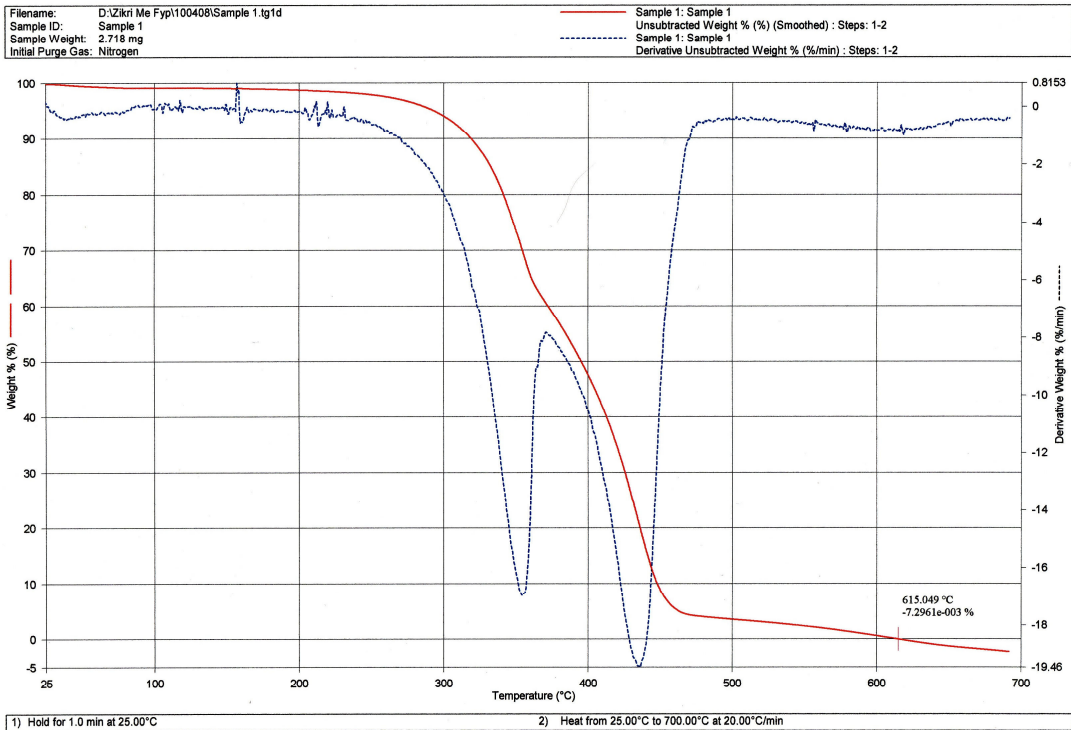


Figure A6a: TGA traces of PU-foam sample 1

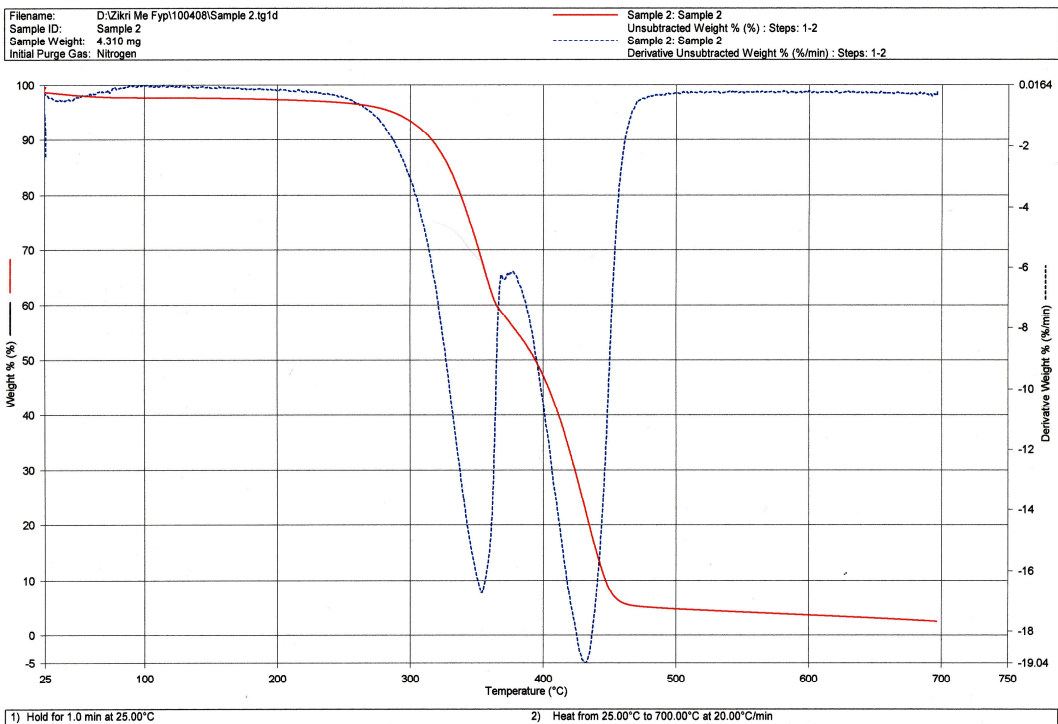
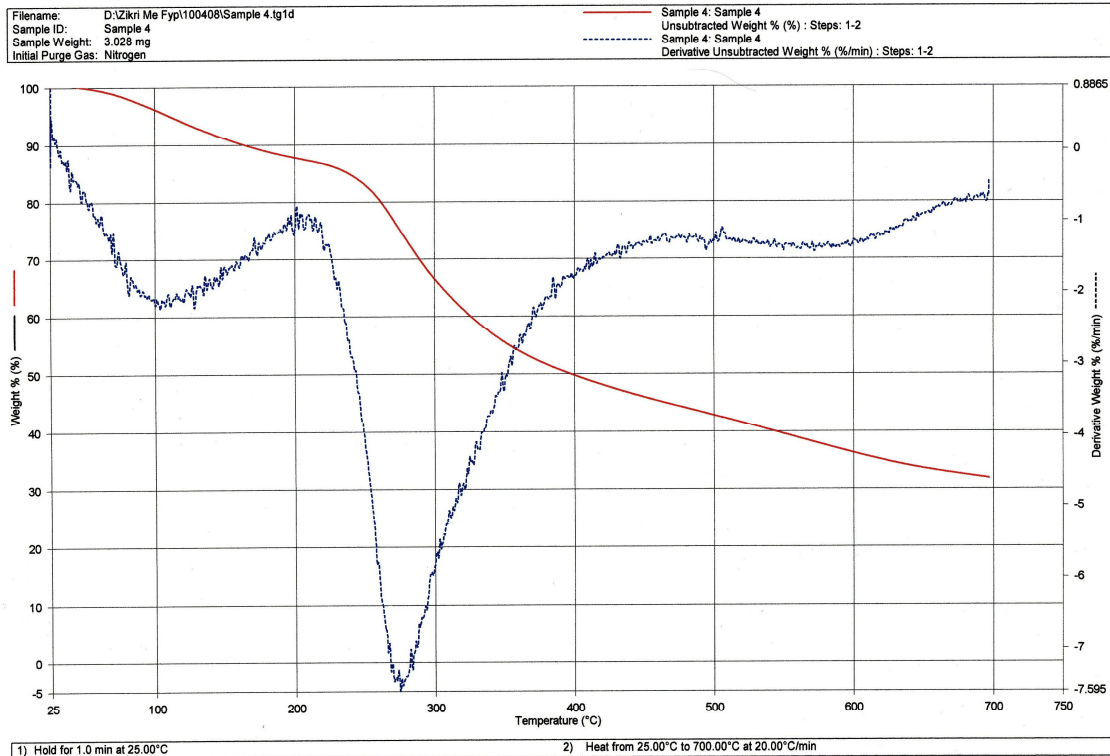
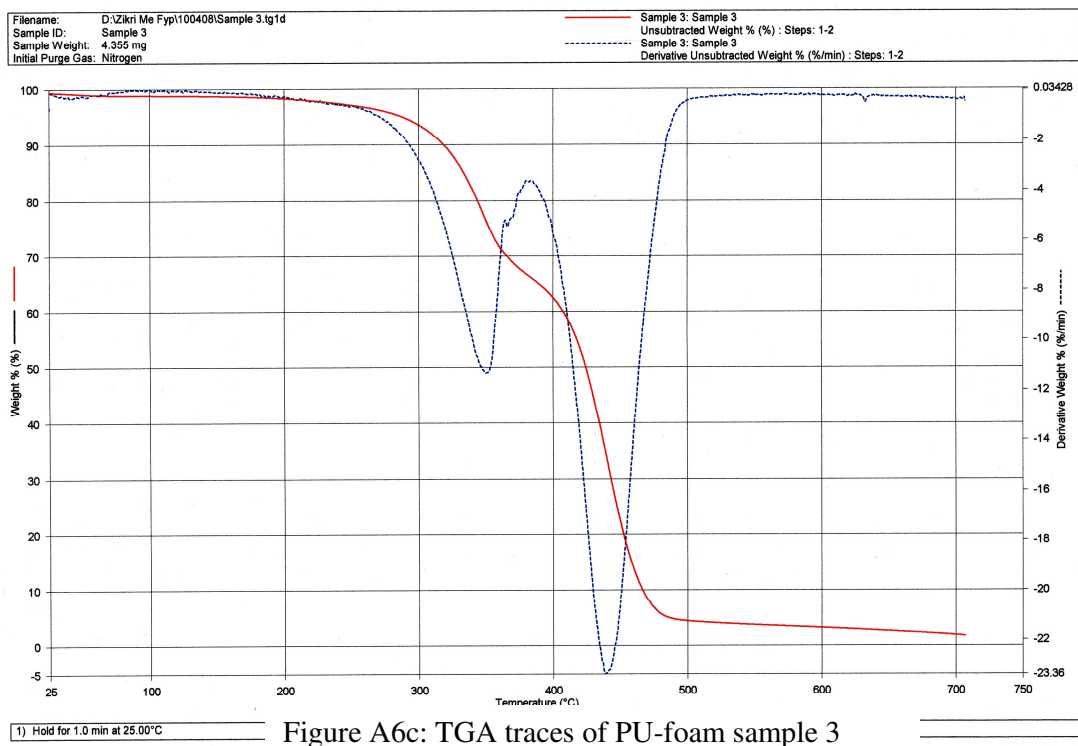


Figure A6b: TGA traces of PU-foam sample 2





## Appendix 7: SEM images of PU-sponge sample

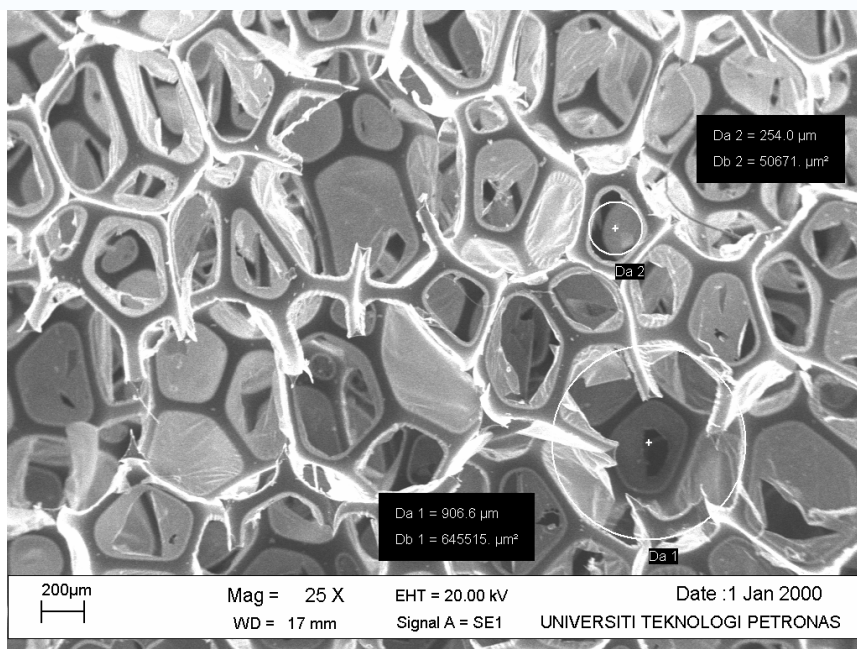


Figure A7a: Image of PU-sponge sample 2

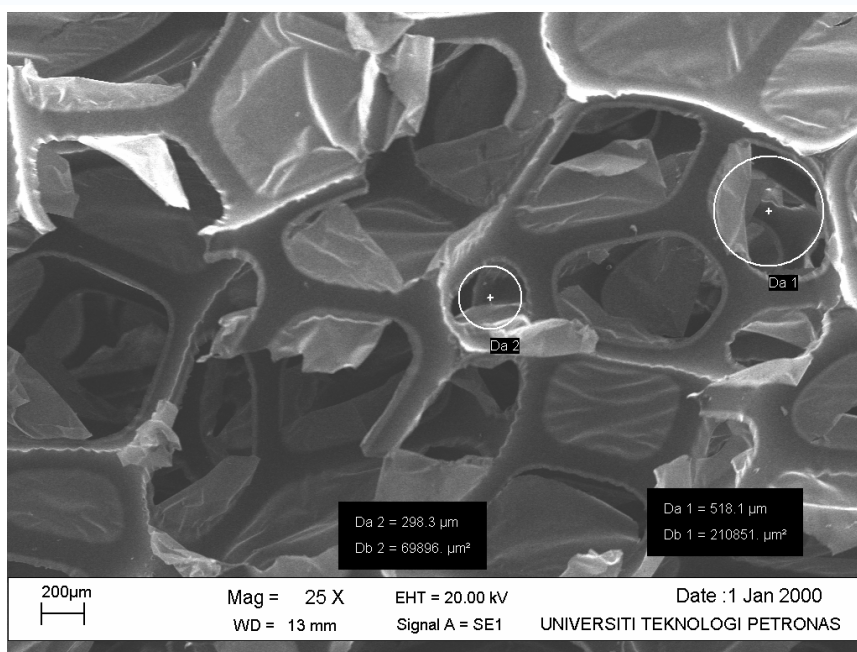


Figure A7b: Image of PU-sponge sample 3



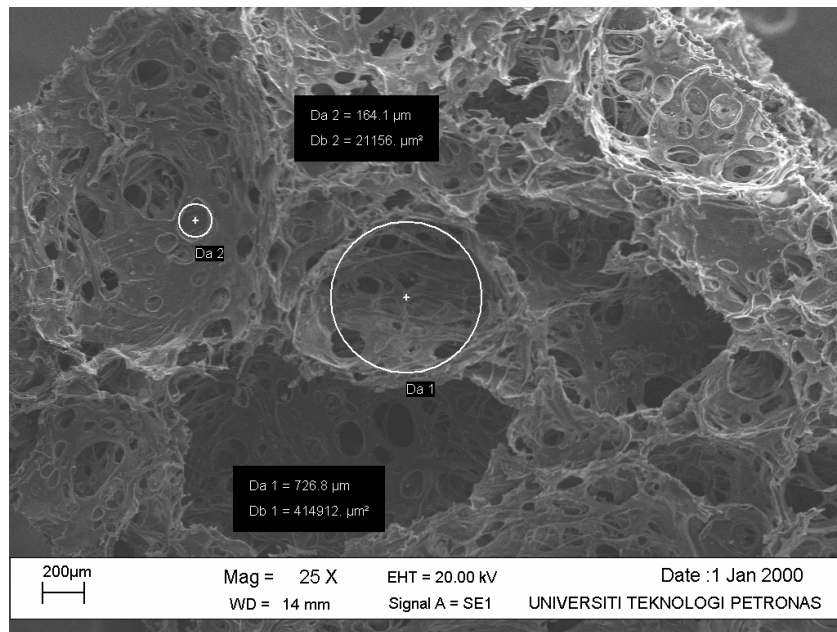


Figure A7c: Image of PU-sponge sample 4

## Appendix 8: Firing schedule for Alumina

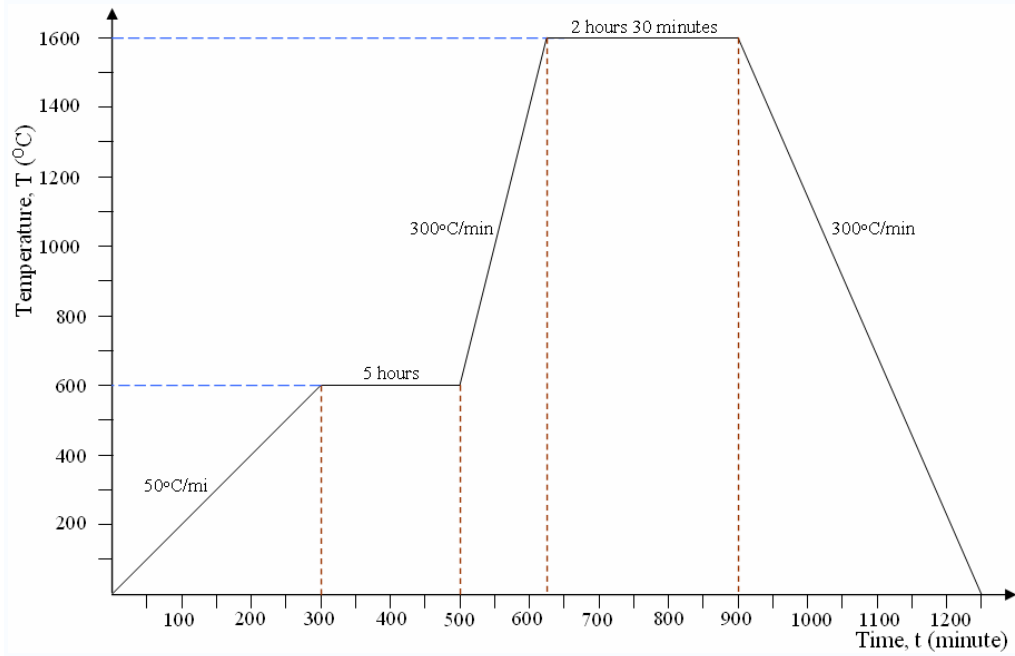


Figure A8: Practiced firing schedule for solid Alumina ceramic